

Contents

IV ELASTICITY	ii
11 Elastostatics	1
11.1 Overview	1
11.2 Displacement and Strain	4
11.2.1 Displacement Vector and its Gradient	4
11.2.2 Expansion, Rotation, Shear and Strain	5
11.3 Stress, Elastic Moduli, and Elastostatic Equilibrium	11
11.3.1 Stress Tensor	11
11.3.2 Realm of Validity for Hooke’s Law	13
11.3.3 Elastic Moduli and Elastostatic Stress Tensor	14
11.3.4 Energy of Deformation	15
11.3.5 Thermoelasticity	17
11.3.6 Molecular Origin of Elastic Stress; Estimate of Moduli	18
11.3.7 Elastostatic Equilibrium: Navier-Cauchy Equation	20
11.4 Young’s Modulus and Poisson’s Ratio for an Isotropic Material: A Simple Elastostatics Problem	23
11.5 Reducing the Elastostatic Equations to One Dimension for a Bent Beam: Cantilever Bridges, Foucault Pendulum, DNA Molecule, Elastica	25
11.6 Buckling and Bifurcation of Equilibria	34
11.6.1 Elementary Theory of Buckling and Bifurcation	34
11.6.2 Collapse of the World Trade Center Buildings	37
11.6.3 Buckling with Lateral Force; Connection to Catastrophe Theory	38
11.6.4 Other Bifurcations: Venus Fly Trap, Whirling Shaft, Triaxial Stars, Onset of Turbulence	39
11.7 Reducing the Elastostatic Equations to Two Dimensions for a Deformed Thin Plate: Stress-Polishing a Telescope Mirror	41
11.8 T2 Cylindrical and Spherical Coordinates: Connection Coefficients and Components of the Gradient of the Displacement Vector	45
11.9 T2 Solving the 3-Dimensional Navier-Cauchy Equation in Cylindrical Coordinates	51
11.9.1 T2 Simple Methods: Pipe Fracture and Torsion Pendulum	51
11.9.2 T2 Separation of Variables and Green’s Functions: Thermoelastic Noise in Mirrors	54

Part IV
ELASTICITY

Elasticity

Version 1211.2.K, 19 Feb 2013

Although ancient civilizations built magnificent pyramids, palaces and cathedrals, and presumably developed insights into how to avoid their collapse, mathematical models for this (the theory of elasticity) were not developed until the 17th century and later.

The 17th-century focus was on a beam (e.g. a vertical building support) under compression or tension. Galileo initiated this study in 1632, followed most notably by Robert Hooke in 1660. Bent beams became the focus with the work of Edme Mariotte in 1680. Bending and compression came together with Leonhard Euler's 1744 theory of the buckling of a compressed beam and his derivation of the complex shapes of very thin wires, whose ends are pushed toward each other (*elastica*). These ideas were extended to two-dimensional thin plates by Marie-Sophie Germain and Joseph-Louis Lagrange in 1811-16, in a study that was brought to full fruition by Augustus Edward Hugh Love in 1888. The full theory of 3-dimensional, stressed, elastic objects was developed by Claude-Louis Navier and by Augustin-Louis Cauchy in 1821-22; and a number of great mathematicians and natural philosophers then developed techniques for solving the Navier-Cauchy equations, particularly for phenomena relevant to railroads and construction. In 1956, with the advent of modern digital computers, M.J. Turner, R.W. Cough, H.C. Martin and L.J. Topp pioneered finite-element methods for numerically modeling stressed bodies. Finite-element numerical simulations are now a standard tool for designing mechanical structures and devices, and, more generally, for solving difficult elasticity problems.

These historical highlights cannot begin to do justice to the history of elasticity research. For much more detail see, e.g., the (out of date) long introduction in Love (1927); and for far more detail than most anyone wants, see the (even more out of date) two-volume work by Todhunter and Pearson (1886).

Despite its centuries-old foundations, elasticity remains of great importance today, and its modern applications include some truly interesting phenomena. Among those applications, most of which we shall touch on in this book, are these: (i) the design and collapse of bridges, skyscrapers, automobiles, and other structures and mechanical devices; (ii) the development and applications of new materials such as carbon nanotubes, which are so light and strong that one could aspire to use them to build a tether connecting a geostationary satellite to the earth's surface; (iii) high-precision physics experiments with torsion pendula and microcantilevers, including brane-worlds-motivated searches for gravitational evidence of macroscopic higher dimensions of space; (iv) nano-scale cantilever probes in scanning electron microscopes and atomic force microscopes; (v) studies of biophysical systems such

as DNA molecules, cell walls, and the Venus fly trap plant; and (vi) plate tectonics, quakes, seismic waves, and seismic tomography in the earth and other planets. Indeed, elastic solids are so central to everyday life and to modern science, that a basic understanding of their behavior should be part of the repertoire of every physicist. That is the goal of this Part IV of our book.

We shall devote just two chapters to elasticity. The first (Chap. 11) will focus on *elastostatics*: the properties of materials and solid objects that are in static equilibrium, with all forces and torques balancing out. The second (Chap. 12) will focus on *elastodynamics*: the dynamical behavior of materials and solid objects that are perturbed away from equilibrium.

Chapter 11

Elastostatics

Version 1211.2.K, 19 Feb 2013

Please send comments, suggestions, and errata via email to kip@caltech.edu or on paper to Kip Thorne, 350-17 Caltech, Pasadena CA 91125

Box 11.1 Reader's Guide

- This chapter relies heavily on the geometric view of Newtonian physics (including vector and tensor analysis) laid out in Chap. 1.
- Chapter 12 (Elastodynamics) is an extension of this chapter; to understand it, this chapter must be mastered.
- The idea of the *irreducible tensorial parts* of a tensor, and its most important example, decomposition of the gradient of a displacement vector into expansion, rotation, and shear (Sec. 11.2.2 and Box 11.2) will be encountered again in Part V (Fluid Mechanics) and Part VI (Plasma Physics).
- Differentiation of vectors and tensors with the help of *connection coefficients* (Sec. 11.8; Track Two), will be used occasionally in Part V (Fluid Mechanics) and Part VI (Plasma Physics), and will be generalized to non-orthonormal bases in Part VII (General Relativity), where it will become Track One and will be used extensively.
- No other portions of this chapter are important for subsequent Parts of this book.

11.1 Overview

In this chapter, we consider static equilibria of elastic solids — for example, the equilibrium shape and internal strains of a steel column in the World Trade Center's Twin Towers, after an airliner crashed into it, and the weight of sagging floors deformed the column (Sec. 11.6).

From the viewpoint of continuum mechanics, a *solid* (e.g. the column's steel) is a substance that recovers its original shape after the application and removal of any *small* stress. Note the requirement that this be true for *any* small stress. Many fluids (e.g. water) satisfy our definition as long as the applied stress is isotropic, but they will deform permanently under a shear stress. Other materials (for example, the earth's crust) are only elastic for limited times, but undergo plastic flow when a small stress is applied for a long time.

We shall focus our attention in this chapter on solids whose deformation (quantified by a *tensorial strain*) is linearly proportional to the applied, small, *tensorial stress*. This linear, three-dimensional stress-strain relationship, which we shall develop and explore in this chapter, generalizes Hooke's famous one-dimensional law (originally expressed in the concise Latin phrase "*Ut tensio, sic vis*"). In English, Hooke's law says that, if an elastic wire or rod is stretched by an applied force F (Fig. 11.1a), its fractional change of length (its strain) is proportional to the force, $\Delta\ell/\ell \propto F$. In the mathematics of stresses and strains (introduced below), Hooke's law says that the longitudinal stress $T_{zz} \equiv$ (longitudinal force F per unit cross sectional area A of the rod) $= F/A$ is proportional to the longitudinal strain $S_{zz} = \Delta\ell/\ell$, with a proportionality constant E called *Young's modulus* that is a property of the material from which the rod is made:

$$\frac{F}{A} \equiv T_{zz} = ES_{zz} \equiv E \frac{\Delta\ell}{\ell} . \quad (11.1)$$

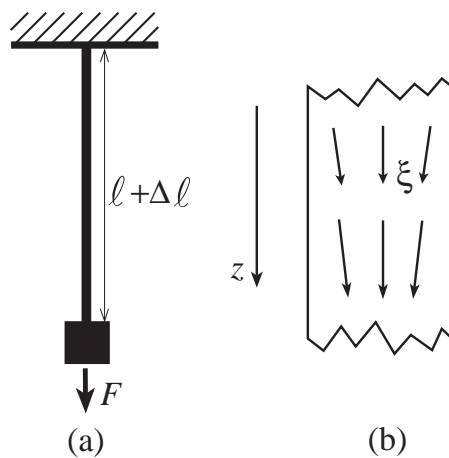


Fig. 11.1: (a) Hooke's one-dimensional law for a rod stretched by a force F : $\Delta\ell/\ell \propto F$. (b) The 3-dimensional displacement vector $\xi(\mathbf{x})$ inside the stretched rod.

Hooke's law turns out to be one component of the three-dimensional stress-strain relation, but in order to understand it deeply in that language, we must first develop a deep understanding of the strain tensor and the stress tensor. Our approach to these tensors will follow the geometric, frame-independent philosophy introduced in Chap. 1. Some readers may wish to review that philosophy and mathematics by rereading or browsing Chap. 1.

We begin our development of elasticity theory in Sec. 11.2 by introducing, in a frame-independent way, the vectorial displacement field $\xi(\mathbf{x})$ inside a stressed body, and its gradient $\nabla\xi$, whose symmetric part is the strain tensor $\mathbf{S} = \nabla\xi$. We then express the strain tensor as the sum of its *irreducible tensorial parts*: an *expansion* Θ and a *shear* Σ .

In Sec. 11.3.1, we introduce the stress tensor and decompose it into its irreducible tensorial parts. In Sec. 11.3.2, we discuss the realms in which there is a linear relationship between stress and strain, and ways in which linearity can fail. In Sec. 11.3.3, assuming linearity we discuss how the material resists volume change (an expansion-type strain) by developing an opposing isotropic stress, with a stress/strain ratio that is equal to the *bulk modulus* K ; and how the material also resists a shear-type strain by developing an opposing shear stress with a stress/strain ratio equal to twice the *shear modulus* 2μ . In Sec. 11.3.4 we evaluate the energy density stored in elastostatic strains, in Sec. 11.3.5 we explore the influence of thermal expansion on the stress-strain relationship, and in Sec. 11.3.6 we discuss the atomic-force origin of the elastostatic stresses and use atomic considerations to estimate the magnitudes of the bulk and shear moduli. Then in Sec. 11.3.7, we compute the elastic force density inside a linear material as the divergence of the sum of its elastic stresses, and we formulate the law of *elastostatic stress balance* (the *Navier-Cauchy equation*) as the vanishing sum of the material's internal elastic force density and any other force densities that may act (usually a gravitational force density due to the weight of the elastic material). We discuss the analogy between this elastostatic stress-balance equation and Maxwell's electrostatic and magnetostatic equations, and we describe how mathematical techniques common in electrostatics (e.g., separation of variables and Green's functions) can also be applied to solve the Navier-Cauchy equation, subject to boundary conditions that describe external forces (e.g. the pull of sagging floors on a steel column).

In Sec. 11.4, we present a simple example of how to solve the three-dimensional Navier-Cauchy equation. Specifically, we use our three-dimensional formulas to deduce Hooke's law for the one-dimensional longitudinal stress and strain in a stretched wire, and we thereby relate Young's modulus E of Hooke's law to the bulk modulus K that resists three-dimensional volume changes, and the shear modulus μ that resists three-dimensional shears.

When the elastic body that one studies is very thin in two dimensions compared to the third (e.g., a wire or rod), we can reduce the three-dimensional elastostatic equations to a set of coupled one-dimensional equations by performing a two-lengthscale expansion. The key to this *dimensional reduction* is taking *moments* of the elastostatic equations. We illustrate this technique in Sec. 11.5, where we treat the bending of beams (e.g. for a cantilevered balcony or bridge or a micron-scale experimental apparatus), and in exercises, where we treat the bending of the support wire of a Foucault pendulum, the bending and stretching of a DNA molecule, and the bending of a very long, thin wire to which forces are applied at the ends (*elastica*).

Elasticity theory, as developed in this chapter, is an example of a common (some would complain far too common) approach to physics problems, namely to linearize them. Linearization may be acceptable when the distortions are small. However, when deformed by sufficiently strong forces, elastic media may become unstable to small displacements, which can then grow to large amplitude, causing rupture. We shall study an example of this in Sec. 11.6: the buckling of a beam or a playing card when subjected to an sufficiently large longitudinal stress. We shall analyze this using our dimensionally reduced, one-dimensional theory. This buckling (as we shall discuss) was central to the collapse of buildings at the World Trade Center on 9/11/01, and it is used by the Venus Fly Trap plant to capture insects. Buckling is associated with *bifurcation of equilibria*, a phenomenon that is common to

many physical systems, not just elastostatic ones. We illustrate bifurcation in Sec. 11.6 using our beam under a compressive load, and we explore its connection to catastrophe theory.

In Sec. 11.7, we discuss dimensional reduction by the method of moments for bodies that are thin in only one dimension, not two; e.g. plates, thin mirrors, and a Venus-fly-trap leaf. In such bodies, the three-dimensional elastostatic equations are reduced to two dimensions. We illustrate our two-dimensional formalism by the stress polishing of telescope mirrors.

Because elasticity theory entails computing gradients of vectors and tensors, and practical calculations are often best performed in cylindrical or spherical coordinate systems, we present a mathematical digression in our Track-two Sec. 11.8 — an introduction to how one can perform practical calculations of gradients of vectors and tensors in the orthonormal bases associated with curvilinear coordinate systems, using the concept of a *connection coefficient* (the directional derivative of one basis vector field along another). In Sec. 11.8 we also use these connection coefficients to derive some useful differentiation formulae in cylindrical and spherical coordinate systems and bases.

As illustrative examples of both connection coefficients and elastostatic force balance, in our Track-Two Sec 11.9 and various exercises, we give practical examples of solutions of the elastostatic force-balance equation in cylindrical coordinates: for a pipe that contains a fluid under pressure (Sec. 11.9.1 and Ex. 11.23); for the wire of a torsion pendulum (Ex. 11.24); and for a cylinder that is subjected to a Gaussian-shaped pressure on one face (Sec. 11.9.2) — a problem central to computing thermal noise in mirrors. We shall sketch how to solve this cylinder-pressure problem using the two common techniques of elastostatics and electrostatics: separation of variables (text of Sec. 11.9.2) and a Green’s function (Ex. 11.26).

11.2 Displacement and Strain

We begin our study of elastostatics by introducing the elastic displacement vector, its gradient, and the irreducible tensorial parts of its gradient. We then identify the strain as the symmetric part of the displacement’s gradient.

11.2.1 Displacement Vector and its Gradient

We label the position of a *point* (a tiny bit of solid) in an unstressed body, relative to some convenient origin in the body, by its position vector \mathbf{x} . Let a force be applied so the body deforms and the point moves from \mathbf{x} to $\mathbf{x} + \boldsymbol{\xi}(\mathbf{x})$; we call $\boldsymbol{\xi}$ the point’s *displacement vector*. If $\boldsymbol{\xi}$ were constant (i.e., if its components in a Cartesian coordinate system were independent of location in the body), then the body would simply be translated and would undergo no deformation. To produce a deformation, we must make the displacement $\boldsymbol{\xi}$ change from one location to another. The most simple, *coordinate-independent* way to quantify those changes is by the *gradient* of $\boldsymbol{\xi}$, $\nabla\boldsymbol{\xi}$. This gradient is a second-rank tensor field;¹ we shall denote it \mathbf{w} :

$$\boxed{\mathbf{w} \equiv \nabla\boldsymbol{\xi}}. \tag{11.2a}$$

¹In our treatment of elasticity theory, we shall make extensive use of the tensorial concepts introduced in Chap. 1.

This tensor is a geometric object, defined independent of any coordinate system in the manner described in Sec. 1.7. In slot-naming index notation (Sec. 1.5), it is denoted

$$W_{ij} = \xi_{i;j} , \quad (11.2b)$$

where the index j after the semicolon is the name of the gradient slot.

In a Cartesian coordinate system the components of the gradient are always just partial derivatives [Eq. (1.15c)], and therefore the Cartesian components of \mathbf{W} are

$$W_{ij} = \frac{\partial \xi_i}{\partial x_j} = \xi_{i,j} . \quad (11.2c)$$

(Recall that indices following a comma represent partial derivatives.) In Sec. 11.8, we shall learn how to compute the components of the gradient in cylindrical and spherical coordinates.

In any small neighborhood of any point \mathbf{x}_o in a deformed body, we can reconstruct the displacement vector $\boldsymbol{\xi}$ from its gradient \mathbf{W} up to an additive constant. Specifically, in Cartesian coordinates, by virtue of a Taylor-series expansion, $\boldsymbol{\xi}$ is given by

$$\begin{aligned} \xi_i(\mathbf{x}) &= \xi_i(\mathbf{x}_o) + (x_j - x_{oj})(\partial \xi_i / \partial x_j) + \dots \\ &= \xi_i(\mathbf{x}_o) + (x_j - x_{oj})W_{ij} + \dots . \end{aligned} \quad (11.3)$$

If we place our origin of Cartesian coordinates at \mathbf{x}_o and let the origin move with the point there as the body deforms [so $\boldsymbol{\xi}(\mathbf{x}_o) = 0$], then Eq. (11.3) becomes

$$\xi_i = W_{ij}x_j \quad \text{when } |\mathbf{x}| \text{ is sufficiently small.} \quad (11.4)$$

We have derived this as a relationship between components of $\boldsymbol{\xi}$, \mathbf{x} , and \mathbf{W} in a Cartesian coordinate system. However, the indices can also be thought of as the names of slots (Sec. 1.5) and correspondingly Eq. (11.4) can be regarded as a geometric, coordinate-independent relationship between the vectors and tensor $\boldsymbol{\xi}$, \mathbf{x} , and \mathbf{W} .

In Ex. 11.2 below, we shall use Eq. (11.4) to gain insight into the displacements associated with various parts of the gradient \mathbf{W} .

11.2.2 Expansion, Rotation, Shear and Strain

In Box 11.2, we introduce the concept of the *irreducible tensorial parts* of a tensor, and we state that in physics, when one encounters a new, unfamiliar tensor, it is often useful to identify the tensor's irreducible parts. The gradient of the displacement vector, $\mathbf{W} = \nabla \boldsymbol{\xi}$ is an important example. It is a second-rank tensor. Therefore, as we discuss in Box 11.2, its irreducible tensorial parts are its trace $\Theta \equiv \text{Tr}(\mathbf{W}) = W_{ii} = \nabla \cdot \boldsymbol{\xi}$, which is called the deformed body's *expansion* for reasons we shall explore below; its symmetric, trace-free part $\boldsymbol{\Sigma}$, which is called the body's *shear*; and its antisymmetric part \mathbf{R} , which is called the body's *rotation*:

$$\boxed{\Theta = W_{ii} = \nabla \cdot \boldsymbol{\xi}} , \quad (11.5a)$$

$$\boxed{\Sigma_{ij} = \frac{1}{2}(W_{ij} + W_{ji}) - \frac{1}{3}\Theta g_{ij} = \frac{1}{2}(\xi_{i;j} + \xi_{j;i}) - \frac{1}{3}\xi_{k;k} g_{ij}} , \quad (11.5b)$$

Box 11.2
Irreducible Tensorial Parts of a Second-Rank Tensor
in 3-Dimensional Euclidean Space

In quantum mechanics, an important role is played by the *rotation group*, i.e., the set of all rotation matrices, viewed as a mathematical entity called a group; see, e.g., Chap. XIII of Messiah (1962) or Chap. 16 of Mathews and Walker (1965). Each tensor in 3-dimensional Euclidean space, when rotated, is said to generate a specific *representation* of the rotation group. Tensors that are “big”, in a sense to be discussed below, can be broken down into a sum of several tensors that are “as small as possible.” These smallest tensors are said to generate *irreducible representations* of the rotation group. All this mumbo-jumbo is really very simple, when one thinks about tensors as geometric, frame-independent objects.

As an example, consider an arbitrary second-rank tensor W_{ij} in three-dimensional, Euclidean space. In the text W_{ij} is the gradient of the displacement vector. From this tensor we can construct the following “smaller” tensors by linear operations that involve only W_{ij} and the metric g_{ij} . (As these smaller tensors are enumerated, the reader should think of the notation used as the basis-independent, frame-independent, slot-naming index notation of Sec. 1.5.1.) The smaller tensors are the contraction (i.e., trace) of W_{ij} ,

$$\Theta \equiv W_{ij}g_{ij} = W_{ii} ; \quad (1)$$

the antisymmetric part of W_{ij}

$$R_{ij} \equiv \frac{1}{2}(W_{ij} - W_{ji}) ; \quad (2)$$

and the symmetric, trace-free part of W_{ij}

$$\Sigma_{ij} \equiv \frac{1}{2}(W_{ij} + W_{ji}) - \frac{1}{3}g_{ij}W_{kk} . \quad (3)$$

It is straightforward to verify that the original tensor W_{ij} can be reconstructed from these three “smaller” tensors, plus the metric g_{ij} as follows:

$$W_{ij} = \frac{1}{3}\Theta g_{ij} + \Sigma_{ij} + R_{ij} . \quad (4)$$

One way to see the sense in which Θ , R_{ij} , and Σ_{ij} are “smaller” than W_{ij} is by counting the number of independent real numbers required to specify their components in an arbitrary basis. (In this counting the reader is asked to think of the index notation as components on a chosen basis.) The original tensor W_{ij} has $3 \times 3 = 9$ components ($W_{11}, W_{12}, W_{13}, W_{21}, \dots$), all of which are independent. By contrast, the 9 components of Σ_{ij} are not independent; symmetry requires that $\Sigma_{ij} \equiv \Sigma_{ji}$, which reduces the number of independent components from 9 to 6; trace-freeness, $\Sigma_{ii} = 0$, reduces it further from 6 to 5. The antisymmetric tensor R_{ij} has just three independent components, R_{12}, R_{23} ,

Box 11.2, Continued

and R_{31} . The scalar Θ has just one. Therefore, (5 independent components in Σ_{ij}) + (3 independent components in R_{ij}) + (1 independent components in Θ) = 9 = (number of independent components in W_{ij}).

The number of independent components (1 for Θ , 3 for R_{ij} , 5 for Σ_{ij}) is a geometric, basis-independent concept: It is the same, regardless of the basis used to count the components; and for each of the “smaller” tensors that make up W_{ij} , it is easily deduced without introducing a basis at all: (Here the reader is asked to think in slot-naming index notation.) The scalar Θ is clearly specified by just one real number. The antisymmetric tensor R_{ij} contains precisely the same amount of information as the vector

$$\phi_i \equiv -\frac{1}{2}\epsilon_{ijk}R_{jk}, \quad (5)$$

as one can see from the fact that Eq. (5) can be inverted to give

$$R_{ij} = -\epsilon_{ijk}\phi_k; \quad (6)$$

and the vector ϕ_i can be characterized by its direction in space (two numbers) plus its length (a third). The symmetric, trace-free tensor Σ_{ij} can be characterized geometrically by the ellipsoid $(g_{ij} + \varepsilon\Sigma_{ij})\zeta_i\zeta_j = 1$, where ε is an arbitrary number $\ll 1$ and ζ_i is a vector whose tail sits at the center of the ellipsoid and head moves around on the ellipsoid’s surface. Because Σ_{ij} is trace-free, this ellipsoid has unit volume. It therefore is specified fully by the direction of its longest principal axis (two numbers) plus the direction of a second principle axis (a third number) plus the ratio of the length of the second axis to the first (a fourth number) plus the ratio of the length of the third axis to the first (a fifth number).

Each of the tensors Θ , R_{ij} (or equivalently ϕ_i), and Σ_{ij} is “irreducible” in the sense that one cannot construct any “smaller” tensors from it, by any linear operation that involves only it, the metric, and the Levi-Civita tensor. Irreducible tensors in 3-dimensional Euclidean space always have an odd number of components. It is conventional to denote this number by $2l + 1$ where the integer l is called the “order of the irreducible representation of the rotation group” that the tensor generates. For Θ , R_{ij} (or equivalently ϕ_i), and Σ_{jk} , l is 0, 1, and 2 respectively. These three tensors can be mapped into the spherical harmonics of order $l = 0, 1, 2$; and their $2l + 1$ components correspond to the $2l + 1$ values of the quantum number $m = -l, -l + 1, \dots, l - 1, l$. For details see, e.g., section II.C of Thorne (1980).

In physics, when one encounters a new, unfamiliar tensor, it is often useful to identify the tensor’s irreducible parts. They almost always play important, independent roles in the physical situation one is studying. We meet one example in this chapter, another when we study fluid mechanics (Chap. 13), and a third in general relativity (Box 25.2).

$$\boxed{R_{ij} = \frac{1}{2}(W_{ij} - W_{ji}) = \frac{1}{2}(\xi_{i;j} - \xi_{j;i})} . \quad (11.5c)$$

Here g_{ij} is the metric, which has components $g_{ij} = \delta_{ij}$ (Kronecker delta) in Cartesian coordinates.

We can reconstruct $\mathbf{W} = \nabla \boldsymbol{\xi}$ from these irreducible tensorial parts in the following manner [Eq. (4) of Box 11.2, rewritten in abstract notation]:

$$\boxed{\nabla \boldsymbol{\xi} = \mathbf{W} = \frac{1}{3}\Theta \mathbf{g} + \boldsymbol{\Sigma} + \mathbf{R}} . \quad (11.6)$$

Let us explore the physical effects of the three separate parts of \mathbf{W} in turn. To understand expansion, consider a small 3-dimensional piece \mathcal{V} of a deformed body (a *volume element*). When the deformation $\mathbf{x} \rightarrow \mathbf{x} + \boldsymbol{\xi}$ occurs, a much smaller element of area² $d\boldsymbol{\Sigma}$ on the surface $\partial\mathcal{V}$ of \mathcal{V} gets displaced through the vectorial distance $\boldsymbol{\xi}$ and in the process sweeps out a volume $\boldsymbol{\xi} \cdot d\boldsymbol{\Sigma}$. Therefore, the change in the volume element's volume, produced by $\boldsymbol{\xi}$, is

$$\delta V = \int_{\partial\mathcal{V}} d\boldsymbol{\Sigma} \cdot \boldsymbol{\xi} = \int_{\mathcal{V}} dV \nabla \cdot \boldsymbol{\xi} = \nabla \cdot \boldsymbol{\xi} \int_{\mathcal{V}} dV = (\nabla \cdot \boldsymbol{\xi})V . \quad (11.7)$$

Here we have invoked Gauss' theorem in the second equality, and in the third we have used the smallness of \mathcal{V} to infer that $\nabla \cdot \boldsymbol{\xi}$ is essentially constant throughout \mathcal{V} and so can be pulled out of the integral. Therefore, the fractional change in volume is equal to the trace of the stress tensor, i.e. the expansion:

$$\boxed{\frac{\delta V}{V} = \nabla \cdot \boldsymbol{\xi} = \Theta} . \quad (11.8)$$

See Figure 11.2 for a simple example.

The shear tensor $\boldsymbol{\Sigma}$ produces the shearing displacements illustrated in Figures 11.2 and 11.3. As it has zero trace, there is no volume change when a body undergoes a pure shear deformation. The shear tensor has five independent components (Box 11.2). However, by rotating our Cartesian coordinates appropriately, we can transform away all the off diagonal elements, leaving only the three diagonal elements Σ_{xx} , Σ_{yy} , Σ_{zz} , which must sum to zero. This is known as a *principal-axis transformation*. Each element produces a stretch ($\Sigma_{..} > 0$ or squeeze ($\Sigma_{..} < 0$) along its axis, and their vanishing sum (the vanishing trace of $\boldsymbol{\Sigma}$) means that there is no net volume change. The components of the shear tensor in any Cartesian

²Note that we use $\boldsymbol{\Sigma}$ for a vectorial area and $\boldsymbol{\Sigma}$ for the shear tensor. There should be no confusion.

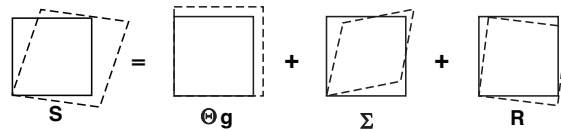


Fig. 11.2: A simple example of the decomposition of a two dimensional distortion of a square body into an expansion (Θ), a shear ($\boldsymbol{\Sigma}$), and a rotation (\mathbf{R}).

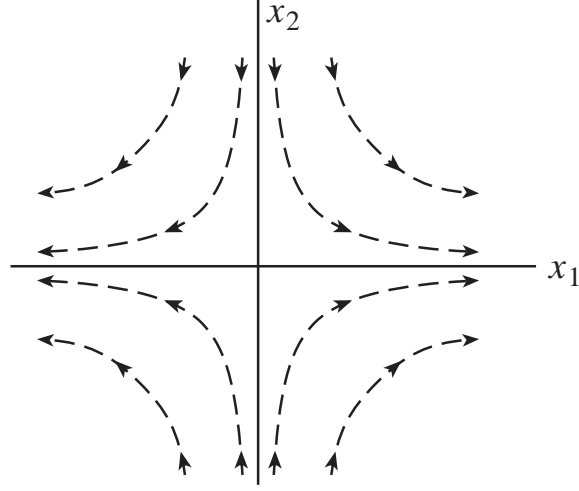


Fig. 11.3: Shear in two dimensions. The displacement of points in a solid undergoing pure shear is the vector field $\boldsymbol{\xi}(\mathbf{x})$ given by Eq. (11.4) with W_{ji} replaced by Σ_{ji} : $\xi_j = \Sigma_{ji}x_i = \Sigma_{j1}x_1 + \Sigma_{j2}x_2$. The integral curves of this vector field are plotted in this figure. The figure is drawn using principal axes, which are Cartesian, so $\Sigma_{12} = \Sigma_{21} = 0$, $\Sigma_{11} = -\Sigma_{22}$, which means that $\xi_1 = \Sigma_{11}x_1$, and $\xi_2 = -\Sigma_{11}x_2$; or, equivalently, $\xi_x = \Sigma_{xx}x$, $\xi_y = -\Sigma_{xx}y$. The integral curves of this simple vector field are the hyperbolae shown in the figure. Note that the displacement increases linearly with distance from the origin. The shear shown in Fig. 11.2 is the same as this, but with the axes rotated counterclockwise by 45 degrees.

coordinate system can be written down immediately from Eq. (11.5b) by substituting the Kronecker delta δ_{ij} for the components of the metric tensor g_{ij} and treating all derivatives as partial derivatives:

$$\Sigma_{xx} = \frac{2}{3} \frac{\partial \xi_x}{\partial x} - \frac{1}{3} \left(\frac{\partial \xi_y}{\partial y} + \frac{\partial \xi_z}{\partial z} \right), \quad \Sigma_{xy} = \frac{1}{2} \left(\frac{\partial \xi_x}{\partial y} + \frac{\partial \xi_y}{\partial x} \right), \quad (11.9)$$

and similarly for the other components. The analogous equations in spherical and cylindrical coordinates will be given in Sec. 11.8 below.

The third term \mathbf{R} in Eq. (11.6) describes a pure rotation which does not deform the solid. To verify this, write $\boldsymbol{\xi} = \boldsymbol{\phi} \times \mathbf{x}$ where $\boldsymbol{\phi}$ is a small rotation of magnitude ϕ about an axis parallel to the direction of $\boldsymbol{\phi}$. Using cartesian coordinates in three dimensional Euclidean space, we can demonstrate by direct calculation that the symmetric part of $\mathbf{W} = \nabla \boldsymbol{\xi}$ vanishes, i.e., $\Theta = \boldsymbol{\Sigma} = 0$, and that

$$R_{ij} = -\epsilon_{ijk} \phi_k, \quad \phi_i = -\frac{1}{2} \epsilon_{ijk} R_{jk}. \quad (11.10a)$$

Therefore the elements of the tensor \mathbf{R} in a cartesian coordinate system just involve the vectoral rotation angle $\boldsymbol{\phi}$. Note that expression (11.10a) for $\boldsymbol{\phi}$ and expression (11.5c) for R_{ij} imply that $\boldsymbol{\phi}$ is half the curl of the displacement vector,

$$\boldsymbol{\phi} = \frac{1}{2} \nabla \times \boldsymbol{\xi}. \quad (11.10b)$$

A simple example of rotation is shown in the last picture in Figure 11.2.

Elastic materials resist expansion Θ and shear Σ , but they don't mind at all having their orientation in space changed; i.e., they do not resist rotations \mathbf{R} . Correspondingly, in elasticity theory, a central focus is on expansion and shear. For this reason, the symmetric part of the gradient of ξ ,

$$S_{ij} \equiv \frac{1}{2}(\xi_{i;j} + \xi_{j;i}) = \Sigma_{ij} + \frac{1}{3}\Theta g_{ij} , \quad (11.11)$$

which includes the expansion and shear but omits the rotation, is given a special name, the *strain*, and is paid great attention.

Let us consider some examples of strains that arise in physical systems.

- (i) Understanding how materials deform under various *loads* (externally applied forces) is central to mechanical, civil and structural engineering. As we shall learn in Sec. 11.3.2 below, all Hookean materials (materials with strain proportional to stress) rupture when the load is so great that any component of their strain exceeds ~ 0.1 , and almost all rupture at strains ~ 0.001 . For this reason, in our treatment of elasticity theory (this chapter and the next), we shall focus on strains that are small compared to unity.
- (ii) Continental drift can be measured on the surface of the earth using Very Long Baseline Interferometry, a technique in which two or more radio telescopes are used to detect interferometric fringes using radio waves from an astronomical point source. (A similar technique uses the Global Positioning System to achieve comparable accuracy.) By observing the fringes, it is possible to detect changes in the spacing between the telescopes as small as a fraction of a wavelength (~ 1 cm). As the telescopes are typically 1000km apart, this means that dimensionless strains $\sim 10^{-8}$ can be measured. Now, the continents drift apart on a timescale $\lesssim 10^8$ yr, so it takes roughly a year for these changes to grow large enough to be measured. Such techniques are also useful for monitoring earthquake faults.
- (iii) The smallest time-varying strains that have been measured so far involve laser interferometer gravitational wave detectors such as LIGO. In each arm of a LIGO interferometer, two mirrors hang freely, separated by 4 km. In 2010 their separations were monitored, at frequencies ~ 100 Hz, to $\sim 10^{-18}$ m, a thousandth the radius of a nucleon³ (Fig. 6.7 with $\xi_{\text{rms}} = \sqrt{f S_F(f)}$). The associated strain is 3×10^{-22} . Although this strain is not associated with an elastic solid, it does indicate the high accuracy of optical measurement techniques.

EXERCISES

³And Advanced LIGO will monitor them with ten times higher accuracy.

Exercise 11.1 *Derivation and Practice: Reconstruction of a Tensor from its Irreducible Tensorial Parts.*

Using Eqs. (1), (2), and (3) of Box 11.2, show that $\frac{1}{3}\Theta g_{ij} + \Sigma_{ij} + R_{ij}$ is equal to W_{ij} .

Exercise 11.2 *Example: The Displacement Vectors Associated with Expansion, Rotation and Shear*

- (a) Consider a $\mathbf{W} = \nabla \boldsymbol{\xi}$ that is pure expansion, $W_{ij} = \frac{1}{3}\Theta g_{ij}$. Using Eq. (11.4) show that, in the vicinity of a chosen point, the displacement vector is $\xi_i = \frac{1}{3}\Theta x_i$. Draw this displacement vector field.
- (b) Similarly, draw $\boldsymbol{\xi}(\mathbf{x})$ for a \mathbf{W} that is pure rotation. [Hint: express $\boldsymbol{\xi}$ in terms of the vectorial angle ϕ with the aid of Eq. (11.10a).]
- (c) Draw $\boldsymbol{\xi}(\mathbf{x})$ for a \mathbf{W} that is pure shear. To simplify the drawing, assume that the shear is confined to the x - y plane, and make your drawing for a shear whose only nonzero components are $\Sigma_{xx} = -\Sigma_{yy}$. Compare your drawing with Fig. 11.3, where the nonzero components are $\Sigma_{xx} = -\Sigma_{yy}$.

11.3 Stress, Elastic Moduli, and Elastostatic Equilibrium

11.3.1 Stress Tensor

The forces acting within an elastic solid are measured by a second rank tensor, the *stress tensor* introduced in Sec. 1.9. Let us recall the definition of this stress tensor:

Consider two small, contiguous regions in a solid. If we take a small element of area $d\boldsymbol{\Sigma}$ in the contact surface with its positive sense⁴ (same as the direction of $d\boldsymbol{\Sigma}$ viewed as a vector) pointing from the first region toward the second, then the first region exerts a force $d\mathbf{F}$ (not necessarily normal to the surface) on the second through this area. The force the second region exerts on the first (through the area $-d\boldsymbol{\Sigma}$) will, by Newton's third law, be equal and opposite to that force. The force and the area of contact are both vectors and there is a linear relationship between them. (If we double the area, we double the force.) The two vectors therefore will be related by a second rank tensor, the stress tensor \mathbf{T} :

$$\boxed{d\mathbf{F} = \mathbf{T} \cdot d\boldsymbol{\Sigma} = \mathbf{T}(\dots, d\boldsymbol{\Sigma}) ; \quad \text{i.e., } dF_i = T_{ij}d\Sigma_j} . \quad (11.12)$$

Thus, the tensor \mathbf{T} is the net (vectorial) force per unit (vectorial) area that a body exerts upon its surroundings. Be aware that many books on elasticity (e.g. Landau and Lifshitz 1986) define the stress tensor with the opposite sign to (11.12). Also be careful not to confuse the shear tensor Σ_{jk} with the vectorial infinitesimal surface area $d\boldsymbol{\Sigma}_j$.

⁴For a discussion of area elements including their positive sense, see Sec. 1.8.

We often need to compute the total elastic force acting on some finite volume \mathcal{V} . To aid in this, we make an important assumption, which we discuss in Sec. 11.3.6, namely that the stress is determined by local conditions and can be computed from the local arrangement of atoms. If this assumption is valid, then (as we shall see in Sec. 11.3.6), we can compute the total force acting on the volume element by integrating the stress over its surface $\partial\mathcal{V}$:

$$\mathbf{F} = - \int_{\partial\mathcal{V}} \mathbf{T} \cdot d\Sigma = - \int_{\mathcal{V}} \nabla \cdot \mathbf{T} dV, \quad (11.13)$$

where we have invoked Gauss' theorem, and the minus sign is because, for a closed surface $\partial\mathcal{V}$ (by convention), $d\Sigma$ points out of \mathcal{V} instead of into it.

Equation (11.13) must be true for arbitrary volumes and so we can identify the *elastic force density* \mathbf{f} acting on an elastic solid as

$$\boxed{\mathbf{f} = -\nabla \cdot \mathbf{T}}. \quad (11.14)$$

In elastostatic equilibrium, this force density must balance all other volume forces acting on the material, most commonly the gravitational force density, so

$$\boxed{\mathbf{f} + \rho\mathbf{g} = 0}, \quad (11.15)$$

where \mathbf{g} is the gravitational acceleration. (Again, there should be no confusion between the vector \mathbf{g} and the metric tensor \mathbf{g} .) There are other possible external forces, some of which we shall encounter later in a fluid context, e.g. an electromagnetic force density. These can be added to Eq. (11.15).

Just as for the strain, the stress tensor \mathbf{T} can be decomposed into its irreducible tensorial parts, a pure trace (the *pressure* P) plus a symmetric trace-free part (the shear stress):

$$\mathbf{T} = P\mathbf{g} + \mathbf{T}^{\text{shear}}; \quad P = \frac{1}{3}\text{Tr}(\mathbf{T}) = \frac{1}{3}T_{ii}. \quad (11.16)$$

There is no antisymmetric part because the stress tensor is symmetric, as we saw in Sec. 1.9. Fluids at rest exert isotropic stresses, i.e. $\mathbf{T} = P\mathbf{g}$. They cannot exert shear stress when at rest, though when moving and shearing they can exert a viscous shear stress, as we shall discuss extensively in Part V (initially Sec. 13.7.2).

In SI units, stress is measured in units of Pascals, denoted Pa

$$1\text{Pa} = 1\text{N/m}^2 = 1\frac{\text{kg m/s}^2}{\text{m}^2}, \quad (11.17)$$

or sometimes in GPa = 10^9 Pa. In cgs units, stress is measured in dyne/cm². Note that 1 Pa = 10 dyne/cm².

Now let us consider some examples of stresses:

- (i) Atmospheric pressure is equal to the weight of the air in a column of unit area extending above the earth, and thus is roughly $P \sim \rho g H \sim 10^5 \text{Pa}$, where $\rho \simeq 1 \text{ kg m}^{-3}$ is the density of air, $g \simeq 10 \text{ m s}^{-2}$ is the acceleration of gravity at the earth's surface, and $H \simeq 10 \text{ km}$ is the atmospheric scale height [$H \equiv (d \ln P / dz)^{-1}$, with z the vertical distance]. Thus 1 atmosphere is $\sim 10^5 \text{ Pa}$ (or, more precisely, $1.01325 \times 10^5 \text{ Pa}$). The stress tensor is isotropic.

- (ii) Suppose we hammer a nail into a block of wood. The hammer might weigh $m \sim 0.3\text{kg}$ and be brought to rest from a speed of $v \sim 10\text{m s}^{-1}$ in a distance of, say, $d \sim 3\text{mm}$. Then the average force exerted on the wood by the nail, as it is driven, is $F \sim mv^2/d \sim 10^4\text{N}$. If this is applied over an effective area $A \sim 1\text{mm}^2$, then the magnitude of the typical stress in the wood is $\sim F/A \sim 10^{10}\text{Pa} \sim 10^5\text{atmosphere}$. There is a large shear component to the stress tensor, which is responsible for separating the fibers in the wood as the nail is hammered.
- (iii) Neutron stars are as massive as the sun, $M \sim 2 \times 10^{30}\text{ kg}$, but have far smaller radii, $R \sim 10\text{km}$. Their surface gravities are therefore $g \sim GM/R^2 \sim 10^{12}\text{m s}^{-2}$, ten billion times that encountered on earth. They have solid crusts of density $\rho \sim 10^{17}\text{kg m}^{-3}$ that are about 1km thick. The magnitude of the stress at the base of a neutron-star crust will then be $P \sim \rho gH \sim 10^{31}\text{Pa}$! This stress will be mainly hydrostatic, though as the material is solid, a modest portion will be in the form of a shear stress.
- (iv) As we shall discuss in Chap. 28, a popular cosmological theory called *inflation* postulates that the universe underwent a period of rapid, exponential expansion during its earliest epochs. This expansion was driven by the stress associated with a *false vacuum*. The action of this stress on the universe can be described quite adequately using a classical stress tensor. If the interaction energy is $E \sim 10^{15}\text{GeV}$, the supposed scale of grand unification, and the associated length scale is the Compton wavelength associated with that energy $l \sim \hbar c/E$, then the magnitude of the stress is $\sim E/l^3 \sim 10^{97}(E/10^{15}\text{GeV})^4\text{ Pa}$.
- (v) Elementary particles interact through forces. Although it makes no sense to describe this interaction using classical elasticity, it does make sense to make order of magnitude estimates of the associated stress. One promising model of these interactions involves *fundamental strings* with mass per unit length $\mu = g_s^2 c^2/8\pi G \sim 0.1\text{ Megaton/Fermi}$ (where Megaton is not the TNT equivalent!), and cross section of order the Planck length squared, $L_P^2 = \hbar G/c^3 \sim 10^{-70}\text{ m}^2$, and tension (negative pressure) $T_{zz} \sim \mu c^2/L_P^2 \sim 10^{110}\text{ Pa}$. Here \hbar , G and c are Planck's (reduced) constant, Newton's gravitation constant, and the speed of light, and $g_s^2 \sim 0.025$ is the string coupling constant.
- (vi) The highest possible stress is presumably associated with spacetime singularities, for example at the birth of the universe or inside a black hole. Here the characteristic energy is the Planck energy $E_P = (\hbar c^5/G)^{1/2} \sim 10^{19}\text{ GeV}$, the lengthscale is the Planck length $L_P = (\hbar G/c^3)^{1/2} \sim 10^{-35}\text{ m}$, and the associated ultimate stress is $\sim E_P/L_P^3 \sim 10^{114}\text{ Pa}$.

11.3.2 Realm of Validity for Hooke's Law

In elasticity theory, motivated by Hooke's Law (Fig. 11.1), we shall assume a linear relationship between a material's stress and strain tensors. Before doing so, however, we shall discuss the realm in which this linearity is true and some ways in which it can fail.

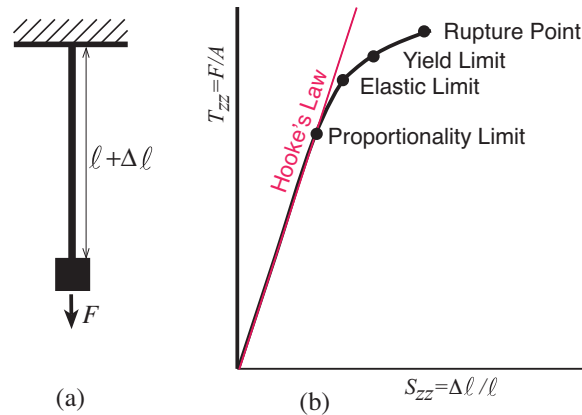


Fig. 11.4: The stress-strain relation for a rod, showing special points at which the behavior of the rod's material changes.

For this purpose, consider, again, the stretching of a rod by an applied force (Fig. 11.1a, shown again here in Fig. 11.4a). For a sufficiently small stress $T_{zz} = F/A$ (with A the cross sectional area of the rod), the strain $S_{zz} = \Delta\ell/\ell$ follows Hooke's law (straight red line in Fig. 11.4b). However, at some point, called the *proportionality limit* (first big dot in Fig. 11.4b), the strain begins to depart from Hooke's law. Despite this deviation, if the stress is removed, the rod returns to its original length. At a bit larger stress, called the *elastic limit*, that ceases to be true; the rod is permanently stretched, somewhat. At a still larger stress, called the *yield limit* or *yield point*, little or no increase in stress causes a large increase in strain, usually because the material begins to flow plastically. At an even larger stress, the *rupture point*, the rod breaks. For a *ductile* substance like polycrystalline copper, the proportionality limit and elastic limit both occur at about the same rather low strain $\Delta\ell/\ell \sim 10^{-4}$, but yield and rupture do not occur until $\Delta\ell/\ell \sim 10^{-3}$. For a more resilient material like cemented tungsten carbide, strains can be proportional and elastic up to $\sim 3 \times 10^{-3}$. Rubber (which is made from a network of cross-linked polymer molecules) is non-Hookean (stress not proportional to strain) at essentially all strains; its proportionality limit is exceedingly small, but it returns to its original shape from essentially all non-rupturing deformations, which can be as large as $\Delta\ell/\ell \sim 8$ (the yield and rupture points).⁵ Especially significant is the fact that in most all solids except rubber, the proportionality, elastic, and yield limits are all very small compared to unity.

11.3.3 Elastic Moduli and Elastostatic Stress Tensor

In realms where Hooke's law is valid, there is a corresponding linear relationship between the material's stress tensor and its strain tensor. The most general linear equation relating two second rank tensors involves a fourth rank tensor known as the *elastic modulus tensor*, \mathbf{Y} . In slot-naming index notation,

$$T_{ij} = -Y_{ijkl}S_{kl} . \quad (11.18)$$

⁵For theoretical explanation of rubber's behavior, see Xing, Goldbart and Radzihovsky (2007).

Now, a general fourth rank tensor in three dimensions has $3^4 = 81$ independent components. Elasticity can get complicated! However, the situation need not be so dire. There are several symmetries that we can exploit. Let us look first at the general case. As the stress and strain tensors are both symmetric, \mathbf{Y} is symmetric in its first pair of slots and we are free to choose it symmetric in its second pair: $Y_{ijkl} = Y_{jikl} = Y_{ijlk}$. There are therefore 6 independent components Y_{ijkl} for variable i, j and fixed k, l , and *vice versa*. In addition, as we show below, \mathbf{Y} is symmetric under an interchange of its first and second pairs of slots: $Y_{ijkl} = Y_{klij}$. There are therefore $(6 \times 7)/2 = 21$ independent components in \mathbf{Y} . This is an improvement over 81. Many substances, notably crystals, exhibit additional symmetries and this can reduce the number of independent components considerably.

The simplest, and in fact most common, case arises when the medium is *isotropic*. In other words, there are no preferred directions in the material. This occurs when the solid is polycrystalline or amorphous and completely disordered on a scale large compared with the atomic spacing, but small compared with the solid's inhomogeneity scale.

If a medium is isotropic, then its elastic properties must be describable by scalars that relate the irreducible parts P and $\mathbf{T}^{\text{shear}}$ of the stress tensor \mathbf{T} to those, Θ and $\mathbf{\Sigma}$, of the strain tensor \mathbf{S} . The only mathematically possible, linear, coordinate-independent relationship between these $\{P, \mathbf{T}^{\text{shear}}\}$ and $\{\Theta, \mathbf{\Sigma}\}$ involving solely scalars is $P = -K\Theta$, $T^{\text{shear}} = -2\mu\mathbf{\Sigma}$, corresponding to a total stress tensor

$$\boxed{\mathbf{T} = -K\Theta\mathbf{g} - 2\mu\mathbf{\Sigma}}. \quad (11.19)$$

Here K is called the *bulk modulus* and μ the *shear modulus*, and the factor 2 is included for purely historical reasons. The first minus sign (with $K > 0$) ensures that the isotropic part of the stress, $-K\Theta\mathbf{g}$, resists volume changes; the second minus sign (with $\mu > 0$) ensures that the symmetric, trace-free part, $-2\mu\mathbf{\Sigma}$, resists shape changes (resists shearing). In Sec. 11.4, we will deduce the relationship of the elastic moduli K and μ to Young's modulus E , which appears in Hooke's law (11.1) for the stress in a stretched rod or fiber (Fig. 11.1).

In many treatments and applications of elasticity, the shear tensor $\mathbf{\Sigma}$ is paid little attention. The focus instead is on the the strain S_{ij} and its trace $S_{kk} = \Theta$, and the elastic stress tensor (11.19) is written as $\mathbf{T} = -\lambda\Theta\mathbf{g} - 2\mu\mathbf{S}$, where $\lambda \equiv K - \frac{2}{3}\mu$. In these treatments μ and λ are called the *first and second Lamé coefficients*, and are used in place of μ and K . We shall not adopt this viewpoint.

11.3.4 Energy of Deformation

Take a wire of length ℓ and cross sectional area A , and stretch it (e.g. via the "Hooke's-law experiment" of Fig. 11.1) by an amount ζ' that grows gradually from 0 to $\Delta\ell$. When the stretch is ζ' , the force that does the stretching is $F' = EA(\zeta'/\ell) = (EV/\ell^2)\zeta'$; here $V = A\ell$ is the wire's volume and E is its Young's modulus. As the wire is gradually lengthened, the stretching force F' does work

$$\begin{aligned} W &= \int_0^{\Delta\ell} F' d\zeta' = \int_0^{\Delta\ell} (EV/\ell^2)\zeta' d\zeta' \\ &= \frac{1}{2}EV(\Delta\ell/\ell)^2. \end{aligned} \quad (11.20)$$

This tells us that the stored elastic energy per unit volume is

$$U = \frac{1}{2}E(\Delta\ell/\ell)^2. \quad (11.21)$$

To generalize this formula to a strained, isotropic, 3-dimensional medium, consider an arbitrary but very small region \mathcal{V} inside a body that has already been strained by a displacement vector field ξ_i and is thus already experiencing an elastic stress $T_{ij} = -K\Theta\delta_{ij} - 2\mu\Sigma_{ij}$ [Eq. (11.19)]. Imagine building up this displacement gradually from zero at the same rate everywhere in and around \mathcal{V} , so at some moment during the buildup the displacement field is $\xi'_i = \xi_i\epsilon$ (with the parameter ϵ gradually growing from 0 to 1). At that moment, the stress tensor (by virtue of the linearity of the stress-strain relation) is $T'_{ij} = T_{ij}\epsilon$. On the boundary $\partial\mathcal{V}$ of the region \mathcal{V} , this stress exerts a force $\Delta F'_i = -T'_{ij}\Delta\Sigma_j$ across any surface element $\Delta\Sigma_j$, from the exterior of $\partial\mathcal{V}$ to its interior. As the displacement grows, this surface force does the following amount of work on \mathcal{V} :

$$\Delta W_{\text{surf}} = \int \Delta F'_i d\xi'_i = \int (-T'_{ij}\Delta\Sigma_j) d\xi'_i = - \int_0^1 T_{ij}\epsilon \Delta\Sigma_j \xi'_i d\epsilon = -\frac{1}{2}T_{ij}\Delta\Sigma_j \xi_i. \quad (11.22)$$

The total amount of work done can be computed by adding up the contributions from all the surface elements of $\partial\mathcal{V}$:

$$W_{\text{surf}} = -\frac{1}{2} \int_{\partial\mathcal{V}} T_{ij}\xi_i d\Sigma_j = -\frac{1}{2} \int_{\mathcal{V}} (T_{ij}\xi_i)_{;j} dV = -\frac{1}{2}(T_{ij}\xi_i)_{;j} V. \quad (11.23)$$

In the second step we have used Gauss's theorem, and in the third step we have used the smallness of the region \mathcal{V} to infer that the integrand is very nearly constant and the integral is the integrand times the total volume V of \mathcal{V} .

Does this equal the elastic energy stored in \mathcal{V} ? The answer is “no”, because we must also take account of the work done in the interior of \mathcal{V} by gravity or any other non-elastic force that may be acting. Now, although it is not easy in practice to turn gravity off and then on, we must do so in this thought experiment: In the volume's final deformed state, the divergence of its elastic stress tensor is equal to the gravitational force density, $\nabla \cdot \mathbf{T} = \rho\mathbf{g}$ [Eqs. (11.14) and (11.15)]; and in the initial, undeformed and unstressed state, $\nabla \cdot \mathbf{T}$ must be zero, whence so must be \mathbf{g} . Therefore, we must imagine growing the gravitational force proportional to ϵ just like we grow the displacement, strain and stress. During this growth, the gravitational force $\rho\mathbf{g}'V = \rho\mathbf{g}V\epsilon$ does the following amount of work on our tiny region \mathcal{V} :

$$W_{\text{grav}} = \int \rho V \mathbf{g}' \cdot d\boldsymbol{\xi}' = \int_0^1 \rho V \mathbf{g}\epsilon \cdot \boldsymbol{\xi} d\epsilon = \frac{1}{2}\rho V \mathbf{g} \cdot \boldsymbol{\xi} = \frac{1}{2}(\nabla \cdot \mathbf{T}) \cdot \boldsymbol{\xi} V = \frac{1}{2}T_{ij;j}\xi_i V. \quad (11.24)$$

The total work done to deform \mathcal{V} is the sum of the work done by the elastic force (11.23) on its surface and the gravitational force (11.24) in its interior, $W_{\text{surf}} + W_{\text{grav}} = -\frac{1}{2}(\xi_i T_{ij})_{;j} V + \frac{1}{2}T_{ij;j}\xi_i V = -\frac{1}{2}T_{ij}\xi_{i;j} V$. This work gets stored in \mathcal{V} as elastic energy, so the energy density is $U = -\frac{1}{2}T_{ij}\xi_{i;j}$. Inserting $T_{ij} = -K\Theta g_{ij} - 2\mu\Sigma_{ij}$ and $\xi_{i;j} = \frac{1}{3}\Theta g_{ij} + \Sigma_{ij} + R_{ij}$

and performing some simple algebra that relies on the symmetry properties of the expansion, shear, and rotation (Ex. 11.3), we obtain

$$U = \frac{1}{2}K\Theta^2 + \mu\Sigma_{ij}\Sigma_{ij}. \quad (11.25)$$

Note that this elastic energy density is always positive if the elastic moduli are positive — as they must be in order that matter be stable to small perturbations.

For the more general, anisotropic case, expression (11.25) becomes [by virtue of the stress-strain relation $T_{ij} = -Y_{ijkl}\xi_{k;l}$, Eq. (11.18)]

$$U = \frac{1}{2}\xi_{i;j}Y_{ijkl}\xi_{k;l}. \quad (11.26)$$

The volume integral of the elastic energy density (11.25) or (11.26) can be used as an action from which to compute the stress, by varying the displacement (Ex. 11.4). Since only the part of \mathbf{Y} that is symmetric under interchange of the first and second pairs of slots contributes to U , only that part can affect the action-principle-derived stress. Therefore, it must be that $Y_{ijkl} = Y_{klij}$. This is the symmetry we asserted earlier.

EXERCISES

Exercise 11.3 *Derivation and Practice: Elastic Energy*

Beginning with $U = -\frac{1}{2}T_{ij}\xi_{i;j}$ [text following Eq. (11.24)], derive $U = \frac{1}{2}K\Theta^2 + \mu\Sigma_{ij}\Sigma_{ij}$ for the elastic energy density inside a body.

Exercise 11.4 *Derivation and Practice: Action Principle for Elastic Stress*

For an anisotropic, elastic medium with elastic energy density $U = \frac{1}{2}\xi_{i;j}Y_{ijkl}\xi_{k;l}$, integrate this energy density over a three-dimensional region \mathcal{V} (not necessarily small) to get the total elastic energy E . Now, consider a small variation $\delta\xi_i$ in the displacement field. Evaluate the resulting change δE in the elastic energy without using the relation $T_{ij} = -Y_{ijkl}\xi_{k;l}$. Convert to a surface integral over $\partial\mathcal{V}$ and therefrom infer the stress-strain relation $T_{ij} = -Y_{ijkl}\xi_{k;l}$.

11.3.5 Thermoelasticity

In our discussion, above, of deformation energy, we tacitly assumed that the temperature of the elastic medium was held fixed during the deformation; i.e., we ignored the possibility of any thermal expansion. Correspondingly, the energy density U that we computed is actually the physical free energy per unit volume \mathcal{F} , at some chosen temperature T_0 of a heat bath. If we increase the bath's and material's temperature from T_0 to $T = T_0 + \delta T$, then the material wants to expand by $\Theta = \delta V/V = 3\alpha\delta T$; i.e., it will have vanishing expansional elastic energy

if Θ has this value. Here α is its coefficient of linear thermal expansion. (The factor 3 is because there are three directions into which it can expand: x , y and z .) Correspondingly, the physical free energy density at temperature $T = T_0 + \delta T$ is

$$\mathcal{F} = \mathcal{F}_0(T) + \frac{1}{2}K(\Theta - 3\alpha\delta T)^2 + \mu\Sigma_{ij}\Sigma_{ij} . \quad (11.27)$$

The stress tensor in this heated and strained state can be computed from $T_{ij} = -\partial\mathcal{F}/\partial S_{ij}$ [a formula most easily inferred from Eq. (11.26) with U reinterpreted as \mathcal{F} and $\xi_{i,j}$ replaced by its symmetrization, S_{ij}]. Reexpressing Eq. (11.27) in terms of S_{ij} and computing the derivative, we obtain (not surprisingly!)

$$T_{ij} = -\frac{\partial\mathcal{F}}{\partial S_{ij}} = -K(\Theta - 3\alpha\delta T)\delta_{ij} - 2\mu\Sigma_{ij} . \quad (11.28)$$

Now, what happens if we allow our material to expand *adiabatically* rather than at fixed temperature? Adiabatic expansion means expansion at fixed entropy S . Consider a small sample of material that contains mass M and has volume $V = M/\rho$. Its entropy is $S = -[\partial(\mathcal{F}V)/\partial T]_V$ [cf. Eq. (5.33)], which, using Eq. (11.27), becomes

$$S = S_0(T) + 3\alpha K\Theta V . \quad (11.29)$$

Here we have neglected the term $-9\alpha^2 K\delta T$, which can be shown to be negligible compared to the temperature dependence of the elasticity-independent term $S_0(T)$. If our sample expands adiabatically by an amount $\Delta V = V\Delta\Theta$, then its temperature must go down by that amount $\Delta T < 0$ which keeps S fixed, i.e. which makes $\Delta S_0 = -3\alpha KV\Delta\Theta$. Noting that $T\Delta S_0$ is the change of the sample's thermal energy, which is $\rho c_V \Delta T$ with c_V the specific heat per unit mass, we see that the temperature change is

$$\frac{\Delta T}{T} = \frac{-3\alpha K\Delta\Theta}{\rho c_V} \quad \text{for adiabatic expansion} . \quad (11.30)$$

This temperature change, accompanying an adiabatic expansion, alters slightly the elastic stress (11.28) and thence the bulk modulus K ; i.e., it gives rise to an adiabatic bulk modulus that differs slightly from the isothermal bulk modulus K introduced in previous sections. However, the differences are so small that they are generally ignored. For further detail see Sec. 6 of Landau and Lifshitz (1986).

11.3.6 Molecular Origin of Elastic Stress; Estimate of Moduli

It is important to understand the microscopic origin of the elastic stress. Consider an ionic solid in which singly ionized ions (e.g. positively charged sodium and negatively charged chlorine) attract their nearest (opposite-species) neighbors through their mutual Coulomb attraction and repel their *next* nearest (same-species) neighbors, and so on. Overall, there is a net electrostatic attraction on each ion, which is balanced by the short range repulsion of its bound electrons against its neighbors' bound electrons. Now consider a thin slice of material of thickness intermediate between the inter-atomic spacing and the solid's inhomogeneity

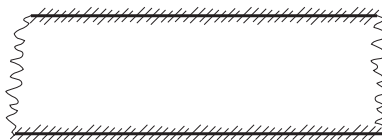


Fig. 11.5: A thin slice of an ionic solid (between the dark lines) that interacts electromagnetically with ions outside it. The electrostatic force on the slice is dominated by interactions between ions lying in the two thin shaded areas, a few atomic layers thick, one on each side of the slice. The force is effectively a surface force rather than a volume force. In elastostatic equilibrium, the forces on the two sides are equal and opposite, if the slice is sufficiently thin.

scale (Fig. 11.5). Although the electrostatic force between individual pairs of ions is long range, the material is electrically neutral on the scale of several ions; and, as a result, when averaged over many ions, the net electric force is of short range (Fig. 11.5). We can therefore treat the net force acting on the thin slice as a surface force, governed by local conditions in the material. This is essential if we are to be able to write down a local, linear stress-strain relation $T_{ij} = -Y_{ijkl}S_{kl}$ or $T_{ij} = -K\theta\delta_{ij} - 2\mu\Sigma_{ij}$. This need not have been the case; there are other circumstances where the net electrostatic force is long range, not short. One example occurs in certain types of crystal (e.g. tourmaline), which develop internal, long-range *piezoelectric* fields when strained.

Our treatment so far has implicitly assumed that matter is continuous on all scales and that derivatives are mathematically well-defined. Of course, this is not the case. In fact, we not only need to acknowledge the existence of atoms, we must also use them to compute the elastic moduli:

We can estimate the elastic moduli in ionic or metallic materials by observing that, if a crystal lattice were to be given a dimensionless strain of order unity, then the elastic stress would be of order the electrostatic force between adjacent ions divided by the area associated with each ion. If the lattice spacing is $a \sim 2\text{\AA} = 0.2\text{ nm}$ and the ions are singly charged, then $K, \mu \sim e^2/4\pi\epsilon_0 a^4 \sim 100\text{ GPa}$. This is about a million atmospheres. Covalently bonded compounds are less tightly bound and have somewhat smaller elastic moduli; and exotic carbon nanotubes have larger moduli. See Table 11.1.

It might be thought, on the basis of this argument, that crystals can be subjected to strains of order unity before they attain their elastic limits. However, as discussed above, most materials are only elastic for strains $\lesssim 10^{-3}$. The reason for this difference is that crystals are generally imperfect and are laced with *dislocations*. Relatively small stresses suffice for the dislocations to move through the solid and for the crystal thereby to undergo permanent deformation (Fig. 11.6).

EXERCISES

Exercise 11.5 *Problem: Order of Magnitude Estimates*

- (a) What is the maximum size of a non-spherical asteroid? [Hint: if the asteroid is too large, its gravity will deform it into a spherical shape.]

Substance	ρ kg m ⁻³	K GPa	μ GPa	E GPa	ν	S_Y	c_L km s ⁻¹	c_T km s ⁻¹
Carbon nanotube	1300			~ 1000		0.05		
Steel	7800	170	81	210	0.29	0.003	5.9	3.2
Copper	8960	130	45	120	0.34	0.0006	4.6	2.2
Rock	3000	70	40	100	0.25		6.	3.5
Glass	2500	47	28	70	0.25	0.0005	5.8	3.3
Rubber	1200	10	0.0007	0.002	0.50	~ 8	1.0	0.03
DNA molecule				0.3		0.03		

Table 11.1: Density ρ ; Bulk, Shear and Young's moduli K , μ and E ; Poisson's ratio ν ; and yield strain S_Y under tension, for various materials. The final two columns are the longitudinal and transverse sound speeds C_L , C_T , defined in Chap. 12. The DNA molecule is discussed in Ex. 11.12.

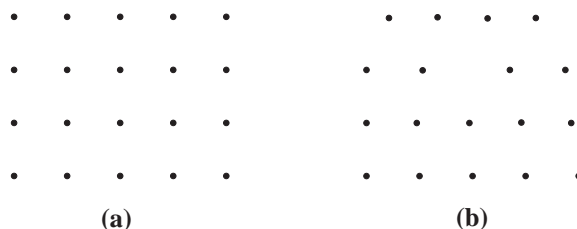


Fig. 11.6: The ions in one layer of a crystal. In subsequent layers, going into each picture, the ion distribution is the same. (a) This perfect crystal, in which the atoms are organized in a perfectly repeating lattice, can develop very large shear strains without yielding. (b) Real materials contain dislocations which greatly reduce their rigidity. The simplest type of dislocation, shown here, is the *edge dislocation* (with the central vertical atomic layer having a terminating edge that extends into the picture). The dislocation will move transversely and the crystal thereby will undergo inelastic deformation when the strain is typically less than $\sim 10^{-3}$, which is one per cent of the yield shear strain for a perfect crystal.

(b) What length of steel wire can hang vertically without breaking? What length of carbon nanotube? What are the prospects to create a tether that hangs to the earth's surface from a geostationary satellite?

(c) Can a helium balloon lift the tank used to transport its helium gas?

Exercise 11.6 Problem: *Jumping Heights*

Explain why all animals, from fleas to humans to elephants, can jump to roughly the same height. The field of science that deals with topics like this is called *allometry*.

11.3.7 Elastostatic Equilibrium: Navier-Cauchy Equation

It is commonly the case that the elastic moduli K and μ are constant, i.e. are independent of location in the medium, even though the medium is stressed in an inhomogeneous way.

(This is because the strains are small and thus perturb the material properties by only small amounts.) If so, then from the elastic stress tensor $\mathbf{T} = -K\Theta\mathbf{g} - 2\mu\boldsymbol{\Sigma}$ and expressions (11.5a) and (11.5b) for the expansion and shear in terms of the displacement vector, we can deduce the following expression for the elastic force density \mathbf{f} [Eq. (11.14)] inside the body:

$$\boxed{\mathbf{f} = -\nabla \cdot \mathbf{T} = K\nabla\Theta + 2\mu\nabla \cdot \boldsymbol{\Sigma} = \left(K + \frac{1}{3}\mu\right) \nabla(\nabla \cdot \boldsymbol{\xi}) + \mu\nabla^2\boldsymbol{\xi}}; \quad (11.31)$$

see Ex. 11.7. Here $\nabla \cdot \boldsymbol{\Sigma}$ in index notation is $\Sigma_{ij;j} = \Sigma_{ji;j}$. Extra terms must be added if we are dealing with anisotropic materials. However, in this book Eq. (11.31) will be sufficient for our needs.

If no other countervailing forces act in the interior of the material (e.g., if there is no gravitational force), and if, as in this chapter, the material is in a static, equilibrium state rather than vibrating dynamically, then this force density will have to vanish throughout the material's interior. This vanishing of $\mathbf{f} \equiv -\nabla \cdot \mathbf{T}$ is just a fancy version of Newton's law for static situations, $\mathbf{F} = m\mathbf{a} = 0$. If the material has density ρ and is pulled on by a gravitational acceleration \mathbf{g} , then the sum of the elastostatic force per unit volume and gravitational force per unit volume must vanish, $\mathbf{f} + \rho\mathbf{g} = 0$; i.e.,

$$\boxed{\mathbf{f} + \rho\mathbf{g} = \left(K + \frac{1}{3}\mu\right) \nabla(\nabla \cdot \boldsymbol{\xi}) + \mu\nabla^2\boldsymbol{\xi} + \rho\mathbf{g} = 0}. \quad (11.32)$$

This is often called the *Navier-Cauchy equation*, since it was first written down by Claude-Louis Navier (in 1821) and in a more general form by Augustin-Louis Cauchy (in 1822).

When external forces are applied to the surface of an elastic body (for example, when one pushes on the face of a cylinder) and gravity acts on the interior, the distribution of the strain $\boldsymbol{\xi}(\mathbf{x})$ inside the body can be computed by solving the Navier-Cauchy equation (11.32) subject to boundary conditions provided by the applied forces.

In electrostatics, one can derive boundary conditions by integrating Maxwell's equations over the interior of a thin box (a "pill box") with parallel faces that snuggle up to the boundary (Fig. 11.7). For example, by integrating $\nabla \cdot \mathbf{E} = \rho_e/\epsilon_0$ over the interior of the pill box, then applying Gauss's law to convert the left side to a surface integral, we obtain the junction condition that the discontinuity in the normal component of the electric field is equal $1/\epsilon_0$ times the surface charge density. Similarly, in elastostatics one can derive boundary conditions by integrating the elastostatic equation $\nabla \cdot \mathbf{T} = 0$ over the pill box of Fig. 11.7 and then applying Gauss's law:

$$0 = \int_V \nabla \cdot \mathbf{T} dV = \int_{\partial V} \mathbf{T} \cdot d\boldsymbol{\Sigma} = \int_{\partial V} \mathbf{T} \cdot \mathbf{n} dA = [(\mathbf{T} \cdot \mathbf{n})_{\text{upper face}} - (\mathbf{T} \cdot \mathbf{n})_{\text{lower face}}]A. \quad (11.33)$$

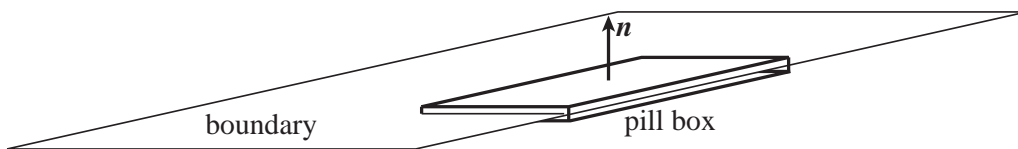


Fig. 11.7: Pill box used to derive boundary conditions in electrostatics and elastostatics.

Here in the next-to-last expression we have used $d\boldsymbol{\Sigma} = \mathbf{n}dA$ where dA is the scalar area element and \mathbf{n} is the unit normal to the pill-box face, and in the last term we have assumed the pill box has a small face so $\mathbf{T} \cdot \mathbf{n}$ can be treated as constant and be pulled outside the integral. The result is the boundary condition that

$$\mathbf{T} \cdot \mathbf{n} \text{ must be continuous across any boundary;} \quad (11.34)$$

i.e., in index notation, $T_{ij}n_j$ is continuous.

Physically this is nothing but the law of force balance across the boundary: *The force per unit area acting from the lower side to the upper side must be equal and opposite to that acting from upper to lower.* As an example, if the upper face is bounded by vacuum then the solid's stress tensor must satisfy $T_{ij}n_j = 0$ at the surface. If a normal pressure P is applied by some external agent at the upper face, then the solid must respond with a normal force equal to P : $n_i T_{ij} n_j = P$. If a vectorial force per unit area \mathcal{F}_i is applied at the upper face by some external agent, then it must be balanced: $T_{ij}n_j = -\mathcal{F}_i$.

Solving the Navier-Cauchy equation (11.33) for the displacement field $\boldsymbol{\xi}(\mathbf{x})$, subject to specified boundary conditions, is a problem in *elastostatics* analogous to solving Maxwell's equations for an electric field subject to boundary conditions in *electrostatics*, or for a magnetic field subject to boundary conditions in *magnetostatics*; and the types of solution techniques used in electrostatics and magnetostatics can also be used here. See Box 11.3.

EXERCISES

Exercise 11.7 *Derivation and Practice: Elastic Force Density*

From Eq. (11.19) derive expression (11.31) for the elastostatic force density inside an elastic body.

Exercise 11.8 *** *Practice: Biharmonic Equation*

A homogeneous, isotropic, elastic solid is in equilibrium under (uniform) gravity and applied surface stresses. Use Eq. (11.31) to show that the displacement inside it $\boldsymbol{\xi}(\mathbf{x})$ is biharmonic, i.e. it satisfies the differential equation

$$\boxed{\nabla^2 \nabla^2 \boldsymbol{\xi} = 0} . \quad (11.35a)$$

Show also that the expansion Θ satisfies the Lapace equation

$$\boxed{\nabla^2 \Theta = 0} . \quad (11.35b)$$

Box 11.3

Methods of Solving the Navier-Cauchy Equation

Many techniques have been devised to solve the Navier-Cauchy equation (11.33), or other equations equivalent to it, subject to appropriate boundary conditions. Among them are:

- *Separation of Variables* (Sec. 11.9.2.)
- *Green's Functions* [Ex. 11.26; Johnson (1985).]
- *Variational Principles* [Chap. 5 of Marsde and Hughes (1983), and Chap. 10 of Slaughter (2002).]
- *Saint-Venant's Principle*, in which one changes the boundary conditions to something simpler, for which the Navier-Cauchy equation can be solved analytically, and then one uses linearity of the Navier-Cauchy equation to compute an approximate, additive correction that accounts for the difference in boundary conditions. Barré de Saint-Venant in 1855 had the insight to realize that, under suitable conditions, the correction will be significant only locally, near the altered boundary, and not globally. [Sec. 2.16 of Ugural and Fenster (2012); and pp. 288 ff of Boresi and Chong (2000) and references therein.]
- *Dimensional Reduction* - to a two-dimensional theory in the case of thin plates (Sec. 11.7), and a one-dimensional theory for rods and for translation-invariant plates (Sec. 11.5).
- *Complex Variable Methods*, which are particularly useful in solving the two-dimensional equations. [Appendix 5B of Boresi and Chong (2000).]
- *Numerical Simulations* on computers. These are usually carried out by the *method of finite elements*, in which one approximates one's stressed objects by a finite set of elementary, interconnected physical elements such as rods; thin, triangular plates; and tetrahedra. [Chap. 7 of Ugural and Fenster (2012).]
- *Replace Navier-Cauchy by Equivalent Equations*. For example, and widely used in the engineering literature: write force balance $T_{ij;j} = 0$ in terms of the strain tensor S_{ij} , supplement this with an equation that guarantees S_{ij} can be written as the symmetrized gradient of a vector field (the displacement vector), and develop techniques to solve these coupled equations plus boundary conditions for S_{ij} . [Sec. 2.4 of Ugural and Fenster (2012); also large parts of Boresi and Chong (2000) and of Slaughter (2002).]
- *Use Mathematica or other computer software* to perform the complicated analytical analyses and explore their predictions numerically. [Constantinescu and Korsunsky (2007).]

11.4 Young's Modulus and Poisson's Ratio for an Isotropic Material: A Simple Elastostatics Problem

As a simple example of an elastostatics problem, we shall explore the connection between our three-dimensional theory of stress and strain, and the one-dimensional Hooke's law [Fig.

11.1 and Eq. (11.1)].

Consider a thin rod of square cross section hanging along the \mathbf{e}_z direction of a Cartesian coordinate system (Fig. 11.1). Subject the rod to a stretching force applied normally and uniformly at its ends. (It could just as easily be a rod under compression.) Its sides are free to expand or contract transversely, since no force acts on them, $dF_i = T_{ij}d\Sigma_j = 0$. As the rod is slender, vanishing of dF_i at its x and y sides implies to high accuracy that the stress components T_{ix} and T_{iy} will vanish throughout the interior; otherwise there would be a very large force density $T_{ij;j}$ inside the rod. Using $T_{ij} = -K\Theta g_{ij} - 2\mu\Sigma_{ij}$, we then obtain

$$T_{xx} = -K\Theta - 2\mu\Sigma_{xx} = 0, \quad (11.36a)$$

$$T_{yy} = -K\Theta - 2\mu\Sigma_{yy} = 0, \quad (11.36b)$$

$$T_{yz} = -2\mu\Sigma_{yz} = 0, \quad (11.36c)$$

$$T_{xz} = -2\mu\Sigma_{xz} = 0, \quad (11.36d)$$

$$T_{xy} = -2\mu\Sigma_{xy} = 0, \quad (11.36e)$$

$$T_{zz} = -K\Theta - 2\mu\Sigma_{zz}. \quad (11.36f)$$

From the first two of these equations and $\Sigma_{xx} + \Sigma_{yy} + \Sigma_{zz} = 0$, we obtain a relationship between the expansion and the nonzero components of the shear,

$$K\Theta = \mu\Sigma_{zz} = -2\mu\Sigma_{xx} = -2\mu\Sigma_{yy}; \quad (11.37)$$

and from this and Eq. (11.36f), we obtain $T_{zz} = -3K\Theta$. The decomposition of S_{ij} into its irreducible tensorial parts tells us that $S_{zz} = \xi_{z;z} = \Sigma_{zz} + \frac{1}{3}\Theta$, which becomes, upon using Eq. (11.37), $\xi_{z;z} = [(3K + \mu)/3\mu]\Theta$. Combining with $T_{zz} = -3K\Theta$ we obtain Hooke's law and an expression for Young's modulus E in terms of the bulk and shear moduli:

$$\frac{-T_{zz}}{\xi_{z;z}} = \frac{9\mu K}{3K + \mu} = E. \quad (11.38)$$

It is conventional to introduce *Poisson's ratio*, ν , which is minus the ratio of the lateral strain to the longitudinal strain during a deformation of this type, where the transverse motion is unconstrained. It can be expressed as a ratio of elastic moduli as follows:

$$\nu \equiv -\frac{\xi_{x,x}}{\xi_{z,z}} = -\frac{\xi_{y,y}}{\xi_{z,z}} = -\frac{\Sigma_{xx} + \frac{1}{3}\Theta}{\Sigma_{zz} + \frac{1}{3}\Theta} = \frac{3K - 2\mu}{2(3K + \mu)}, \quad (11.39)$$

where we have used Eq. (11.37). We tabulate these and their inverses for future use:

$$\boxed{E = \frac{9\mu K}{3K + \mu}, \quad \nu = \frac{3K - 2\mu}{2(3K + \mu)}; \quad K = \frac{E}{3(1 - 2\nu)}, \quad \mu = \frac{E}{2(1 + \nu)}}. \quad (11.40)$$

We have already remarked that mechanical stability of a solid requires that $K, \mu > 0$. Using Eq. (11.40), we observe that this imposes a restriction on Poisson's ratio, namely that $-1 < \nu < 1/2$. For metals, Poisson's ratio is typically about $1/3$ and the shear modulus is roughly half the bulk modulus. For a substance that is easily sheared but not easily

compressed, like rubber, the bulk modulus is relatively high and $\nu \simeq 1/2$ (cf. Table 11.1.) For some exotic materials, Poisson's ratio can be negative (cf. Yeganeh-Haeri *et al* 1992).

Although we derived them for a square strut under compression, our expressions for Young's modulus and Poisson's ratio are quite general. To see this, observe that the derivation would be unaffected if we combined many parallel, square fibers together. All that is necessary is that the transverse motion be free so that the only applied force is uniform and normal to a pair of parallel faces.

11.5 Reducing the Elastostatic Equations to One Dimension for a Bent Beam: Cantilever Bridges, Foucault Pendulum, DNA Molecule, Elastica

When dealing with bodies that are much thinner in two dimensions than the third (e.g. rods, wires, and beams), one can use the *method of moments* to reduce the three-dimensional elastostatic equations to ordinary differential equations in one dimension (a process called *dimensional reduction*). We have already met an almost trivial example of this in our discussion of Hooke's law and Young's modulus (Sec. 11.4 and Fig. 11.1). In this section, we shall discuss a more complicated example, the bending of a beam through a small displacement angle; and in Ex. 11.13 we shall analyze a more complicated example: the bending of a very long, elastic wire into a complicated shape called an *elastica*.

Our beam-bending example is motivated by a common method of bridge construction, which uses cantilevers. (A famous historical example is the old bridge over the Firth of Forth in Scotland that was completed in 1890 with a main span of half a km.) The principle is to attach two independent beams to the two shores as cantilevers, and allow them to meet in the middle. (In practice the beams are usually supported at the shores on piers and strengthened along their lengths with trusses.) Similar cantilevers, with lengths of order a micron or less, are used in scanning electron microscopes, atomic force microscopes, and other nanotechnology applications, including quantum information experiments.

Let us make a simple model of a cantilever (Figure 11.8). Consider a beam clamped rigidly at one end, with length ℓ , horizontal width w and vertical thickness h . Introduce local cartesian coordinates with \mathbf{e}_x pointing along the beam and \mathbf{e}_z pointing vertically upward. Imagine the beam extending horizontally in the absence of gravity. Now let it sag under its own weight so that each element is displaced through a small distance $\boldsymbol{\xi}(\mathbf{x})$. The upper part of the beam is stretched while the lower part is compressed, so there must be a *neutral surface* where the horizontal strain $\xi_{x,x}$ vanishes. This neutral surface must itself be curved downward. Let its downward displacement from the horizontal plane that it occupied before sagging be $\eta(x) (> 0)$, let a plane tangent to the neutral surface make an angle $\theta(x)$ (also > 0) with the horizontal, and adjust the x and z coordinates so x runs along the slightly curved neutral plane and z is orthogonal to it (Fig. 11.8). The longitudinal strain is then given to first order in small quantities by

$$\xi_{x,x} = \frac{z}{\mathcal{R}} = z \frac{d\theta}{dx} \simeq z \frac{d^2\eta}{dx^2}, \quad (11.41a)$$

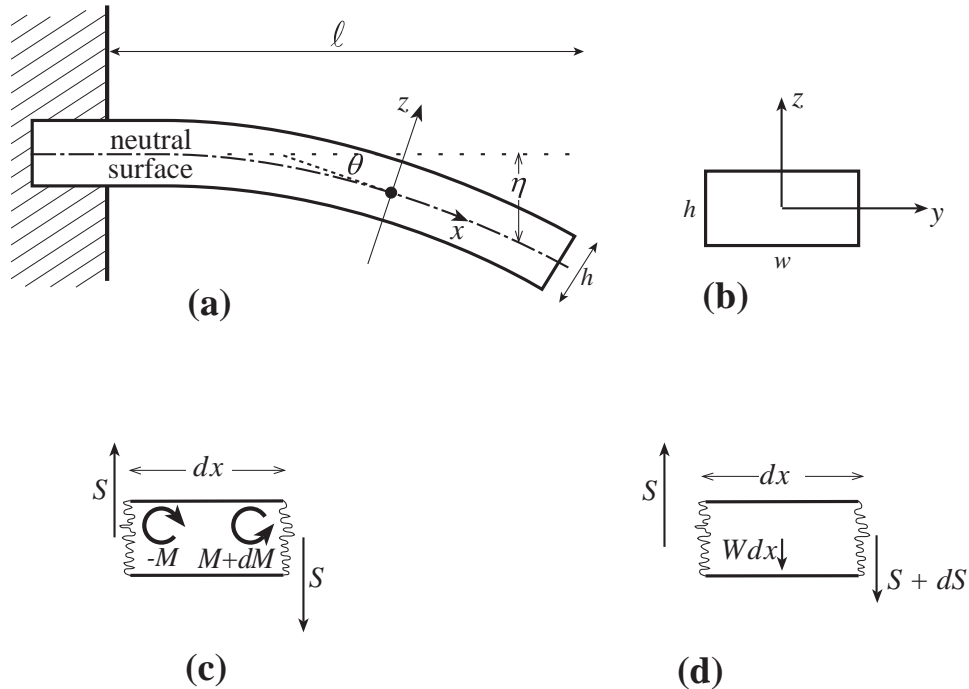


Fig. 11.8: Bending of a cantilever. (a) A beam is held rigidly at one end and extends horizontally with the other end free. We introduce an orthonormal coordinate system (x, y, z) with \mathbf{e}_x extending along the beam. We only consider small departures from equilibrium. The bottom of the beam will be compressed, the upper portion extended. There is therefore a neutral surface $z = 0$ on which the strain $\xi_{x,x}$ vanishes. (b) The beam has a rectangular cross section with horizontal width w and vertical thickness h ; its length is ℓ . (c) The bending torque M must be balanced by the torque exerted by the vertical shearing force S . (d) S must vary along the beam so as to support the beam's weight per unit length, W .

where $\mathcal{R} = dx/d\theta > 0$ is the radius of curvature of the beam's bend and we have chosen $z = 0$ at the neutral surface. The one-dimensional displacement $\eta(x)$ will be the focus for dimensional reduction of the elastostatic equations.

As in our discussion of Hooke's law for a stretched rod (Sec. 11.4), we can regard the beam as composed of a bundle of long, parallel fibers, stretched or squeezed along their length, and free to contract transversely. The longitudinal stress is therefore

$$T_{xx} = -E\xi_{x,x} = -Ez \frac{d^2\eta}{dx^2}. \quad (11.41b)$$

We can now compute the horizontal force density, which must vanish in elastostatic

equilibrium⁶

$$f_x = -T_{xx,x} - T_{xz,z} = Ez \frac{d^3\eta}{dx^3} - T_{xz,z} = 0. \quad (11.41c)$$

This is a partial differential equation. We convert it into a one-dimensional ordinary differential equation by the *method of moments*: We multiply it by z and integrate over z (i.e., we compute its “first moment”). Integrating the second term, $\int zT_{xz,z}dz$, by parts and using the boundary condition $T_{xz} = 0$ on the upper and lower surfaces of the beam, we obtain

$$\frac{Eh^3}{12} \frac{d^3\eta}{dx^3} = - \int_{-h/2}^{h/2} T_{xz} dz. \quad (11.41d)$$

Notice (using $T_{xz} = T_{zx}$) that the integral, when multiplied by the beam’s width w in the y direction, is the vertical *shearing force* $S(x)$ in the beam:

$$S = \int T_{zx} dy dz = w \int_{-h/2}^{h/2} T_{zx} dz = -D \frac{d^3\eta}{dx^3}. \quad (11.42a)$$

Here

$$D \equiv E \int z^2 dy dz \equiv EA r_g^2 = Ewh^3/12 \quad (11.42b)$$

is called the beam’s *flexural rigidity*, or its *bending modulus*. Notice that, quite generally, D is the beam’s Young’s modulus E times the second moment of the beam’s cross sectional area A . Engineers call that second moment Ar_g^2 and they call r_g the radius of gyration. For our rectangular beam, this D is $Ewh^3/12$.

As an aside, we can gain some insight into Eq. (11.42a) by examining the torques that act on a segment of the beam with length dx . As shown in Fig. 11.8c, the shear forces on the two ends of the segment exert a clockwise torque $2S(dx/2) = Sdx$. This is balanced by a counterclockwise torque due to the stretching of the upper half of the segment and compression of the lower half, i.e. due to the bending of the beam. This bending torque is

$$M \equiv \int T_{xx} z dy dz = -D \frac{d^2\eta}{dx^2} \quad (11.42c)$$

on the right end of the segment and minus this on the left, so torque balance says $(dM/dx)dx = Sdx$, i.e.

$$S = dM/dx; \quad (11.43)$$

see Fig. 11.8c. This is precisely Eq. (11.42a).

⁶Because the coordinates are slightly curvilinear rather than precisely Cartesian, our Cartesian-based analysis makes small errors. Track-two readers who have studied Sec. 11.8 below can evaluate those errors using connection coefficient terms that were omitted from this equation: $-\Gamma_{xjk}T_{jk} - \Gamma_{jkj}T_{xk}$. Each Γ has magnitude $1/\mathcal{R}$ so these terms are of order T_{jk}/\mathcal{R} , whereas the terms kept in Eq. (11.41c) are of order T_{xx}/ℓ and T_{xz}/h ; and since the thickness h and length ℓ of the beam are small compared to the beam’s radius of curvature \mathcal{R} , the connection-coefficient terms are negligible.

Equation (11.42a) [or equivalently (11.43)] embodies half of the elastostatic equations. It is the x component of force balance $f_x = 0$, converted to an ordinary differential equation by evaluating its lowest non-vanishing moment: its first moment, $\int z f_x dy dz = 0$ [Eq. (11.41d)]. The other half is the z component of stress balance, which we can write as

$$T_{zx,x} + T_{zz,z} + \rho g = 0 \quad (11.44)$$

(vertical elastic force balanced by gravitational pull on the beam). We can convert this to a one-dimensional ordinary differential equation by taking its lowest nonvanishing moment, its zero'th moment, i.e. by integrating over y and z . The result is

$$\boxed{\frac{dS}{dx} = -W}, \quad (11.45)$$

where $W = g\rho wh$ is the beam's weight per unit length (Fig. 11.8d).

Combining our two dimensionally reduced components of force balance, Eqs. (11.42a) and (11.45), we obtain a fourth order differential equation for our one-dimensional displacement $\eta(x)$:

$$\boxed{\frac{d^4\eta}{dx^4} = \frac{W}{D}}. \quad (11.46)$$

(Fourth order differential equations are characteristic of elasticity.)

Equation (11.46) can be solved subject to four appropriate boundary conditions. However, before we solve it, notice that *for a beam of a fixed length ℓ , the deflection η is inversely proportional to the flexural rigidity*. Let us give a simple example of this scaling. Floors in American homes are conventionally supported by wooden joists of 2" (inch) by 6" lumber with the 6" side vertical. Suppose an inept carpenter installed the joists with the 6" side horizontal. The flexural rigidity of the joist would be reduced by a factor 9 and the center of the floor would be expected to sag 9 times as much as if the joists had been properly installed – a potentially catastrophic error.

Also, before solving Eq. (11.46), let us examine the approximations that we have made. First, we have assumed that the sag is small compared with the length of the beam, when making the small-angle approximation in Eq. (11.41a); and we have assumed the beam's radius of curvature is large compared to its length, when treating our slightly curved coordinates as Cartesian.⁷ These assumptions will usually be valid, but are not so for the elastica studied in Ex. 11.13. Second, by using the method of moments rather than solving for the complete local stress tensor field, we have ignored the effects of some components of the stress tensor. In particular, in evaluating the bending torque [Eq. (11.42c)] we have ignored the effect of the T_{zx} component of the stress tensor. This is $O(h/\ell)T_{xx}$ and so our equations can only be accurate for fairly slender beams. Third, the extension above the neutral surface and the compression below the neutral surface lead to changes in the cross sectional shape of the beam. The fractional error here is of order the longitudinal shear, which is small for real materials.

⁷i.e., in more technical language, when neglecting the connection coefficient terms discussed in footnote 6.

The solution to Eq. (11.46) is a fourth order polynomial with four unknown constants, to be set by boundary conditions. In this problem, the beam is held horizontal at the fixed end so that $\eta(0) = \eta'(0) = 0$, where $' = d/dx$. At the free end, T_{zx} and T_{xx} must vanish, so the shearing force S must vanish, whence $\eta'''(\ell) = 0$ [Eq. (11.42a)]; and the bending torque M [Eq. (11.42c)] must also vanish, whence [by Eq. (11.43)] $\int S dx \propto \eta''(\ell) = 0$. By imposing these four boundary conditions $\eta(0) = \eta'(0) = \eta''(\ell) = \eta'''(\ell) = 0$ on the solution of Eq. (11.46), we obtain for the beam shape

$$\eta(x) = \frac{W}{D} \left(\frac{1}{4}\ell^2 x^2 - \frac{1}{6}\ell x^3 + \frac{1}{24}x^4 \right). \quad (11.47a)$$

Therefore the end of the beam sags by

$$\eta(\ell) = \frac{W\ell^4}{8D}. \quad (11.47b)$$

Problems in which the beam rests on supports rather than being clamped can be solved in a similar manner. The boundary conditions will be altered, but the differential equation (11.46) will be unchanged.

Now suppose that we have a cantilever bridge of constant vertical thickness h and total span $2\ell \sim 100\text{m}$ made of material with density $\rho \sim 8 \times 10^3 \text{kg m}^{-3}$ (e.g. reinforced concrete) and Young's modulus $E \sim 100\text{GPa}$. Suppose further that we want the center of the bridge to sag by no more than $\eta \sim 1\text{m}$. According to Eq. (11.47b), the thickness of the beam must satisfy

$$h \gtrsim \left(\frac{3\rho g \ell^4}{2E\eta} \right)^{1/2} \sim 2.7\text{m}. \quad (11.48)$$

This estimate makes no allowance for all the extra strengthening and support present in real structures (e.g. via trusses and cables) and so it is an overestimate.

EXERCISES

Exercise 11.9 *Derivation: Sag in a cantilever*

- Verify Eqs. (11.47) for the sag in a horizontal beam clamped at one end and allowed to hang freely at the other end.
- Now consider a similar beam with constant cross section and loaded with weights so that the total weight per unit length is $W(x)$. What is the sag of the free end, expressed as an integral over $W(x)$, weighted by an appropriate Green's function?

Exercise 11.10 *Example: Microcantilever*

A microcantilever, fabricated from a single crystal of silicon, is being used to test the inverse square law of gravity on micron scales (Weld et. al. 2008). It is clamped horizontally at

one end and its horizontal length is $\ell = 300\mu\text{m}$, its horizontal width is $w = 12\mu\text{m}$ and its vertical height is $h = 1\mu\text{m}$. (The density and Young's modulus for silicon are $\rho = 2000\text{kg m}^{-3}$, $E = 100\text{ GPa}$ respectively.) The cantilever is loaded at its free end with a $M = 10\mu\text{g}$ gold mass.

- Show that the static deflection of the end of the cantilever is $\eta(\ell) = Mg\ell^3/3D = 9\mu\text{m}$, where $g = 10\text{ m s}^{-2}$ is the acceleration due to gravity. Explain why it is permissible to ignore the weight of the cantilever.
- Next suppose the mass is displaced slightly vertically and then released. Show that the natural frequency of oscillation of the cantilever is $f = (1/2\pi)\sqrt{g/\eta(\ell)} \simeq 200\text{Hz}$.
- A second, similar mass is placed $100\mu\text{m}$ away from the first mass. Estimate roughly the Newtonian gravitational attraction between these two masses and compare with the attraction of the Earth. Suggest a method that exploits the the natural oscillation of the cantilever to measure the tiny gravitational attraction of the two gold masses.

Exercise 11.11 *Example: Foucault Pendulum*

In any high-precision Foucault pendulum, it is important that the pendular restoring force be isotropic, since anisotropy will make the swinging period be different in different planes and thereby will cause precession of the plane of swing. The answer to the elastica exercise 11.13 can be adapted to model the effect of anisotropy on the pendulum's period.

- Consider a pendulum of mass m and length ℓ suspended as shown in Figure 11.9 by a rectangular wire with thickness h in the plane of the bend ($X - Z$ plane) and thickness w orthogonal to that plane (Y direction). Explain why the force that the wire exerts on the mass is $-\mathbf{F} = -(mg \cos \theta_o + m\ell\dot{\theta}_o^2)\mathbf{e}_x$, where g is the acceleration of gravity, θ_o is defined in the figure, $\dot{\theta}_o$ is the time derivative of θ_o due to the swinging of the pendulum, and in the second term we have assumed that the wire is long compared to its region of bend. Express the second term in terms of the amplitude of swing θ_o^{max} , and show that for small amplitudes $\theta_o^{\text{max}} \ll 1$, $\mathbf{F} \simeq -mg\mathbf{e}_x$. Use this approximation in the subsequent parts.

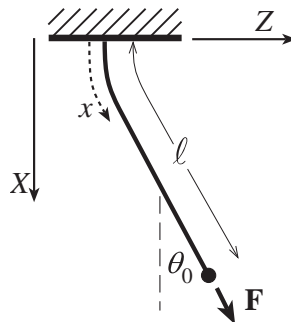


Fig. 11.9: Foucault Pendulum

- (b) Assuming that all along the wire, its angle $\theta(x)$ to the vertical is small, $\theta \ll 1$, show that

$$\theta(x) = \theta_o[1 - e^{-x/\lambda}] , \quad (11.49a)$$

where λ (not to be confused with the second Lamé coefficient) is

$$\lambda = \frac{h}{(12\epsilon)^{1/2}} , \quad (11.49b)$$

$\epsilon = \xi_{x,x}$ is the longitudinal strain in the wire, and h is the wire's thickness in the plane of its bend. Note that the bending of the wire is concentrated near the support, so this is where dissipation will be most important and where most of the suspension's thermal noise will arise (cf. Sec. 6.8 for discussion of thermal noise).

- (c) Hence show that the shape of the wire is given in terms of cartesian coordinates by

$$Z = [X - \lambda(1 - e^{-X/\lambda})]\theta_o , \quad (11.49c)$$

and that the pendulum period is

$$P = 2\pi \left(\frac{\ell - \lambda}{g} \right)^{1/2} . \quad (11.49d)$$

- (d) Finally show that the pendulum periods when swinging along \mathbf{e}_x and \mathbf{e}_y differ by

$$\frac{\delta P}{P} = \left(\frac{h - w}{\ell} \right) \left(\frac{1}{48\epsilon} \right)^{1/2} . \quad (11.49e)$$

From this one can determine how accurately the two thicknesses h and w must be equal to achieve a desired degree of isotropy in the period. A similar analysis can be carried out for the more realistic case of a slightly elliptical wire.

Exercise 11.12 *Example: DNA Molecule—Bending, Stretching, Young's Modulus and Yield Point*

A DNA molecule consists of two long strands wound around each other as a helix, forming a cylinder with radius $a \simeq 1$ nm. In this exercise, we shall explore three ways of measuring the molecule's Young's modulus E . For background and further details, see Marko and Cocco (2003), and Chap. 9 of Nelson (2004).

- (a) Show that, if a segment of DNA with length ℓ is bent into a segment of a circle with radius R , its elastic energy is $E_{\text{el}} = D\ell/2R^2$, where $D = (\pi/4)a^4E$ is the molecule's flexural rigidity.
- (b) Biophysicists define the DNA's *persistence length* ℓ_p as that length which, when bent through an angle of 90° , has elastic energy $E_{\text{el}} = k_B T$, where k_B is Boltzmann's constant and T is the temperature of the molecule's environment. Show that $\ell_p \simeq D/k_B T$. Explain why, in a thermalized environment, segments much shorter than ℓ_p will be more or less straight, and segments with length $\sim \ell_p$ will be randomly bent through angles of order 90° .

- (c) Explain why a DNA molecule with total length L will usually be found in a random coil with diameter $d \simeq \ell_p \sqrt{L/\ell_p} = \sqrt{L\ell_p}$. Observations at room temperature with $L \simeq 17\mu\text{m}$ reveal that $d \simeq 1\mu\text{m}$. From this show that the persistence length is $\ell_p \simeq 50$ nm at room temperature, and thence evaluate the molecule's flexural rigidity and from it, show that the molecule's Young's modulus is $E \simeq 0.3$ GPa; cf. Table 11.1.
- (d) When the ends of a DNA molecule are attached to glass beads and the beads are pulled apart with a gradually increasing force F , the molecule begins to uncoil. To understand this semiquantitatively, think of the molecule as like a chain made of N links, each with length ℓ_p , whose interfaces can bend freely. If the force acts along the z direction, explain why the probability that any chosen link will make an angle θ to the z axis is $dP/d\cos\theta \propto \exp(+F\ell_p \cos\theta/k_B T)$. [Hint: this is analogous to the probability $dP/dV \propto \exp(-PV/k_B T)$ for the volume V of a system in contact with a bath that has pressure P and temperature T [Eq. (5.49)]; see also the discussion preceding Eq. (11.57) below.] Infer, then, that when the force is F , the molecule's length along the force's direction is $\bar{L} = N\ell_p \tanh(F\ell_p/k_B T)$. This tells us that for $F \ll k_B T/\ell_p \sim 0.1$ pN, the molecule will have a linear force-length relation, with spring constant $dF/d\bar{L} = k_B T/(L\ell_p) \propto T^2$ (where $L = N\ell_p$ is the molecule's length when straightened out).⁸ By measuring the spring constant, one can infer that $\ell_p \simeq 35$ nm (roughly the same as the 50 nm inferred from the rms size of the coiled molecule at zero force), and thence that $E \simeq 0.2$ GPa.
- (e) When $F \gg k_B T/\ell_p \sim 0.1$ pN, the crude jointed-chain model predicts that the molecule is stretched to its full length $L = N\ell_p$. At this point, its true elasticity should take over and allow genuine stretching. That true elasticity turns out to dominate only for forces $\gtrsim 10$ pN. [For details of what happens between 0.1 and 10 pN see, e.g., Secs. 9.1–9.4 of Nelson (2004).] For a force between ~ 10 and ~ 80 pN, the molecule is measured to obey Hooke's law, with a Young's modulus $E \simeq 0.3$ GPa that agrees with the value inferred from its random-coil diameter. When the applied force reaches $\simeq 80$ pN, the molecule's double helix suddenly begins to unwind and stretch greatly with small increases of force, so this is the molecule's *yield point*. Show that the strain at this yield point is $\Delta\ell/\ell \simeq 0.03$; cf. Table 11.1.

Exercise 11.13 *** *Example: Elastica*

Consider a slender wire of rectangular cross section resting on a horizontal surface (so gravity is unimportant), with horizontal thickness h and vertical thickness w . Let the wire be bent in the horizontal plane (so gravity is unimportant) as a result of equal and opposite forces F that act at its ends; Fig. 11.10. The various shapes the wire can assume are called *elastica*; they were first computed by Euler in 1744 and are discussed on pp. 401–404 of Love (1927). The differential equation that governs the wire's shape is similar to that for the cantilever, Eq. (11.46), with the simplification that the wire's weight does not enter the problem and the complication that the wire is long enough to deform through large angles.

⁸Rubber is made of long, polymeric molecules, and its elasticity arises from this same kind of uncoiling of the molecules when a force is applied, and as here, its spring constant is temperature dependent, and for the same reason.

It is convenient (as in the cantilever problem, Fig. 11.8) to introduce curvilinear coordinates with coordinate x measuring distance along the neutral surface, z measuring distance orthogonal to x in the plane of the bend (horizontal plane), and y measured perpendicular to the bending plane (vertically). The unit vectors along the x , y , and z directions are \mathbf{e}_x , \mathbf{e}_y , \mathbf{e}_z (Figure 11.10). Let $\theta(x)$ be the angle between \mathbf{e}_x and the applied force \mathbf{F} ; $\theta(x)$ is determined, of course, by force and torque balance.

- (a) Show that force balance along the x and z directions implies

$$F \cos \theta = \int T_{xx} dydz, \quad F \sin \theta = \int T_{zx} dydz \equiv S. \quad (11.50a)$$

- (b) Show that torque balance for a short segment of wire implies

$$S = \frac{dM}{dx}, \quad \text{where } M(x) \equiv \int z T_{xx} dydz \text{ is the bending torque.} \quad (11.50b)$$

- (c) Show that the stress-strain relation in the wire implies

$$M = -D \frac{d\theta}{dx}, \quad (11.50c)$$

where $D = Ewh^3/12$ is the flexural rigidity, Eq. (11.42b).

- (d) From the above relations, derive the following differential equation for the shape of the wire:

$$\boxed{\frac{d^2\theta}{dx^2} = -\frac{F \sin \theta}{D}}. \quad (11.50d)$$

This is the same equation as describes the motion of a simple pendulum!

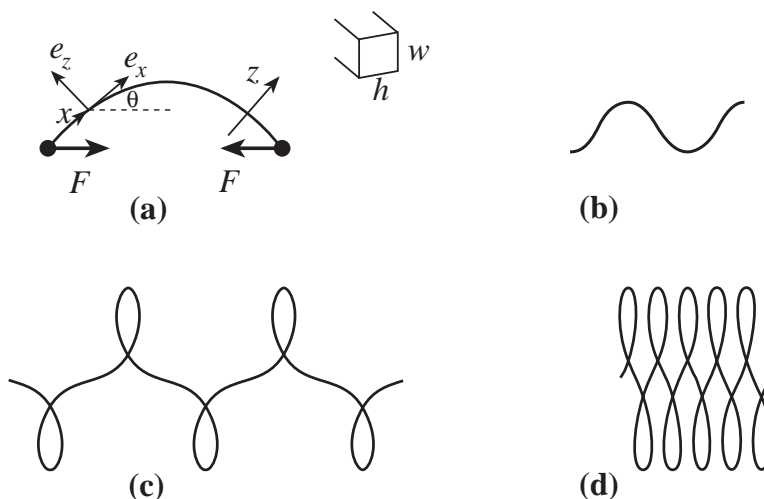


Fig. 11.10: Elastica. (a) A bent wire is in elastostatic equilibrium under the action of equal and opposite forces applied at its two ends. x measures distance along the neutral surface; z measures distance orthogonal to the wire in the plane of the bend. (b), (c), (d) Examples of the resulting shapes.

- (e) For track-two readers who have studied Sec. 11.8: Go back through your analysis and identify any place that connection coefficients would enter into a more careful computation, and explain why the connection-coefficient terms are negligible.
- (f) Find one non-trivial solution of the elastica equation (11.50d) either analytically using elliptic integrals or numerically. (The general solution can be expressed in terms of elliptic integrals.)
- (g) Solve analytically or numerically for the shape adopted by the wire corresponding to your solution in (f), in terms of precisely Cartesian coordinates (X, Z) in the bending (horizontal) plane. Hint: express the curvature of the wire, $1/\mathcal{R} = d\theta/dx$ as

$$\frac{d\theta}{dx} = \frac{d^2 X}{dZ^2} \left[1 + \left(\frac{dX}{dZ} \right)^2 \right]^{-3/2}. \quad (11.50e)$$

- (h) Obtain a uniform piece of wire and adjust the force \mathbf{F} to compare your answer with experiment.

11.6 Buckling and Bifurcation of Equilibria

So far, we have considered stable elastostatic equilibria, and have implicitly assumed that the only reason for failure of a material is exceeding the yield limit. However, anyone who has built a house of cards knows that mechanical equilibria can be unstable, with startling consequences. In this section, we shall explore a specific, important example of a mechanical instability: *buckling* — the theory of which was developed long ago, in 1744 by Leonard Euler.

A tragic example of buckling was the collapse of the World Trade Center's twin towers on September 11, 2001. We shall discuss it near the end of this section, after first developing the theory in the context of a much simpler and cleaner example:

11.6.1 Elementary Theory of Buckling and Bifurcation

Take a new playing card and squeeze it between your finger and thumb (Figure 11.11). When you squeeze gently, the card remains flat, but when you gradually increase the compressive force F past a critical value F_{crit} , the card suddenly buckles, i.e. bends; and the curvature of the bend then increases rather rapidly with increasing applied force.

To understand quantitatively the sudden onset of buckling, we derive an eigenequation for the transverse displacement η as a function of distance x from one end of the card. (Although the card is effectively two dimensional, it has translation symmetry along its

transverse dimension, so we can use the one-dimensional equations of Sec. 11.5.) We suppose that the ends are free to pivot but not move, so

$$\eta(0) = \eta(\ell) = 0 . \quad (11.51)$$

For small displacements, the bending torque of our dimensionally-reduced one-dimensional theory is [Eq. (11.42c)]

$$M(x) = -D \frac{d^2 \eta}{dx^2} , \quad (11.52)$$

where $D = wh^3E/12$ is the flexural rigidity [Eq. (11.42b)]. As the card is very light (negligible gravity), the total torque around location x , acting on a section of the card from x to one end, is the bending torque $M(x)$ acting at x plus the torque $-F\eta(x)$ associated with the applied force, and this sum must vanish:

$$D \frac{d^2 \eta}{dx^2} + F\eta = 0 . \quad (11.53)$$

The eigensolutions of Eq. (11.53) satisfying boundary conditions (11.51) are

$$\eta = \eta_0 \sin kx , \quad (11.54a)$$

with eigenvalues

$$k = \left(\frac{F}{D} \right)^{1/2} = \frac{n\pi}{\ell} \quad \text{for non-negative integers } n. \quad (11.54b)$$

Therefore, there is a critical force (first derived by Leonhard Euler in 1744), given by

$$F_{\text{crit}} = \frac{\pi^2 D}{\ell^2} = \frac{\pi^2 wh^3 E}{12 \ell^2} . \quad (11.55)$$

When $F < F_{\text{crit}}$, there is no solution except $\eta = 0$ (an unbent card). When $F = F_{\text{crit}}$, the unbent card is still a solution, and there suddenly is the additional, arched solution (11.54) with $n = 1$, depicted in Fig. 11.11.

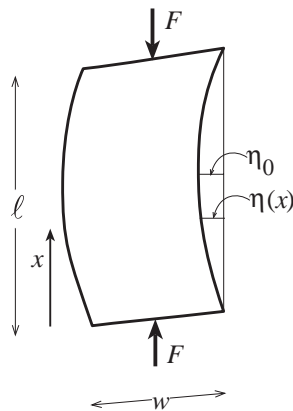


Fig. 11.11: A playing card of length ℓ , width w and thickness h is subjected to a compressive force F , applied at both ends. The ends of the card are fixed but are free to pivot.

The linear approximation, which we have used, cannot tell us the height η_0 of the arch as a function of F for $F \geq F_{\text{crit}}$; it reports, incorrectly, that for $F = F_{\text{crit}}$ all arch heights are allowed, and that for $F > F_{\text{crit}}$ there is no solution with $n = 1$. However, when nonlinearities are taken into account (Ex. 11.14), we learn that the $n = 1$ solution continues to exist for $F > F_{\text{crit}}$, and the arch height η_0 is related to F by

$$F = F_{\text{crit}} \left\{ 1 + \frac{1}{2} \left(\frac{\pi\eta_0}{2\ell} \right)^2 + \mathcal{O} \left[\left(\frac{\pi\eta_0}{2\ell} \right)^4 \right] \right\} . \quad (11.56)$$

The sudden appearance of the arched equilibrium state as F is increased through F_{crit} is called a *bifurcation of equilibria*. This bifurcation also shows up in the elastodynamics of the playing card, as we shall deduce in Sec. 12.3.5. When $F < F_{\text{crit}}$, small perturbations of the card's unbent shape oscillate stably. When $F = F_{\text{crit}}$, the unbent card is neutrally stable, and its zero-frequency motion leads the card from its unbent equilibrium state to its $n = 1$, arched equilibrium. When $F > F_{\text{crit}}$, the straight card is an unstable equilibrium: its $n = 1$ perturbations grow in time, driving the card toward the $n = 1$ arched equilibrium state.

A nice way of looking at this bifurcation is in terms of free energy. Consider candidate equilibrium states labeled by the height η_0 of their arch. For each value of η_0 , give the card (for concreteness) the $n = 1$ sine-wave shape $\eta = \eta_0 \sin(\pi x/\ell)$. Compute the total elastic energy $E(\eta_0)$ associated with the card's bending and subtract off the work $F\delta X$ done on the card by the applied force F when the card arches from $\eta_0 = 0$ to height η_0 . (Here $\delta X(\eta_0)$ is the arch-induced decrease in straight-line separation between the card's ends). The resulting quantity, $V(\eta_0) = E - F\delta X$ is the card's *free energy* — analogous to the physical free energy $F = E - TS$ for a system in contact with a heat bath (Secs. 5.4.1 and 11.3.5) and the Gibbs (chemical) free energy $G = E - TS + PV$ when in contact with a heat and pressure bath (Sec. 5.5). It is the relevant energy for analyzing the card's equilibrium and dynamics, when the force F is continually being applied at the two ends. In Ex. (11.15) we deduce that this free energy is

$$V = \left(\frac{\pi\eta_0}{2\ell} \right)^2 \ell \left[(F_{\text{crit}} - F) + \frac{1}{4} F_{\text{crit}} \left(\frac{\pi\eta_0}{2\ell} \right)^2 \right] + \mathcal{O} \left[F_{\text{crit}} \ell \left(\frac{\pi\eta_0}{2\ell} \right)^6 \right] , \quad (11.57)$$

which we depict in Fig. 11.12.

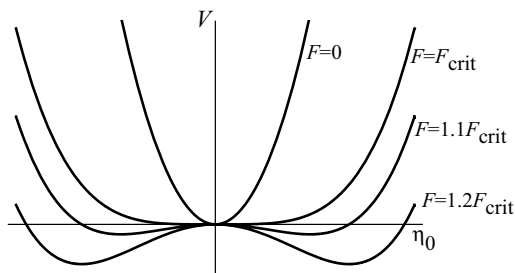


Fig. 11.12: Representation of bifurcation by a potential energy function $V(\eta_0)$. (a) When the applied force is small, there is only one stable equilibrium. (b) As the applied force F is increased, the bottom of the potential well flattens and eventually the number of equilibria increases from one to three, of which only two are stable.

At small values of the compressive force F [curve (a)], the free energy has only one minimum $\eta_0 = 0$ corresponding to a single stable equilibrium, the straight card. However, as the force is increased through F_{crit} , the potential minimum flattens out and then becomes a maximum flanked by two new minima [curve (b)]. The maximum for $F > F_{\text{crit}}$ is the unstable, zero-displacement (straight-card) equilibrium and the two minima are the two stable, finite-amplitude equilibria with positive and negative η_0 given by Eq. (11.56).

This procedure of representing a continuous system with an infinite number of degrees of freedom by just one or a few coordinates and finding the equilibrium by minimizing a free energy is quite common and powerful.

Thus far, we have discussed only two of the card's equilibrium shapes (11.54): the straight shape $n = 0$ and the single-arch shape $n = 1$. *If the card were constrained, by gentle, lateral stabilizing forces, to remain straight beyond $F = F_{\text{crit}}$, then at $F = n^2 F_{\text{crit}}$ for each $n = 2, 3, 4, \dots$, the n 'th order perturbative mode, with $\eta = \eta_0 \sin(n\pi x/\ell)$, would become unstable, and a new, stable equilibrium with this shape would bifurcate from the straight equilibrium. You can easily explore this for $n = 2$ using a playing card.*

These higher-order modes are rarely of practical importance. In the case of a beam with no lateral constraints, as F increases above F_{crit} , it will buckle into its single-arched shape, and then, for beam dimensions commonly used in construction, a fairly modest further increase of F will bend it enough that its yield point and then rupture point are reached. To experience this yourself, take a thin meter stick, compress its ends between your two hands, and see what happens.

11.6.2 Collapse of the World Trade Center Buildings

We return, now, to the example with which we began this section. On September 11, 2001, al-Qaeda operatives hijacked two Boeing 767 passenger airplanes and crashed them into the 110-story twin towers of the World Trade Center in New York City, triggering the towers' collapse a few hours later, with horrendous loss of life.

The weight of a tall building such as the towers is supported by vertical steel beams, called *columns*. The longer the column, the lower the weight it can support without buckling, since $F_{\text{crit}} = \pi^2 D/\ell^2 = \pi^2 EA(r_g/\ell)^2$ with A the beam's cross sectional area, r_g its radius of gyration, and ℓ its length [Eqs. (11.55) and (11.42b)]. The column lengths are typically chosen such that the critical stress for buckling, $F_{\text{crit}}/A = E(\pi r_g/\ell)^2$, is roughly the same as the yield stress, $F_{\text{yield}} \simeq 0.003E$ (cf. Table 11.1), which means that the columns' *slenderness ratio* is $\ell/r_g \sim 50$. The columns are physically far longer than $50r_g$, but they are anchored to each other laterally every $\sim 50r_g$ by beams and girders in the floors, so their effective length for buckling is $\ell \sim 50r_g$. The columns' radii of gyration r_g are generally made large, without using more steel than needed to support the overhead weight, by making the columns hollow, or giving them H shapes. In the twin towers, the thinnest beams had $r_g \sim 13$ cm and they were anchored in every floor, with floor separations $\ell \simeq 3.8$ m, so their slenderness ratio was actually $\ell/r_g \simeq 30$.

According to a detailed investigation [NIST (2005); especially Secs. 6.14.2 and 6.14.3], the crashing airplanes ignited fires in and near floors 93–99 of the North Tower and 78–83 of the South Tower, where the airplanes hit. The fires were most intense in the floors and

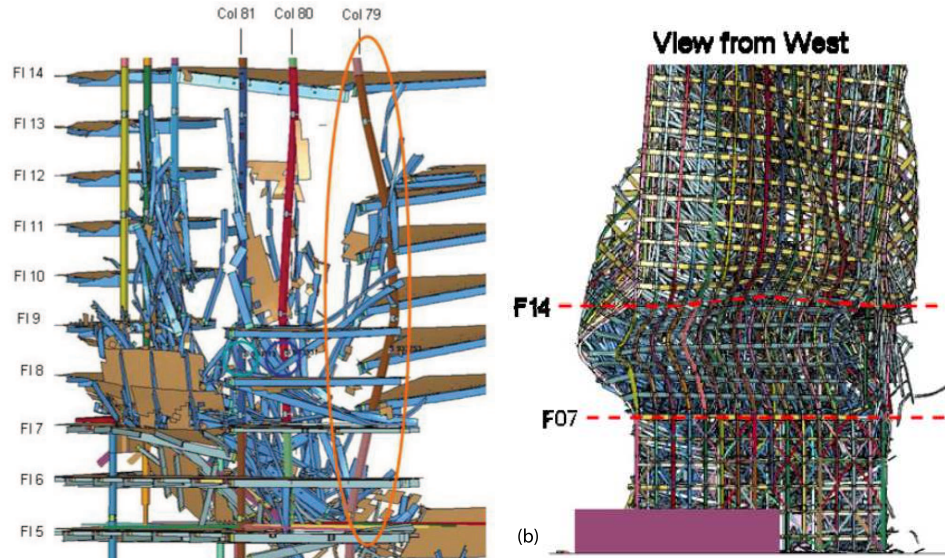


Fig. 11.13: (a) The buckling of column 79 in building WTC7 at the World Trade Center, based on a finite-element simulation informed by all available observational data. (b) The subsequent buckling of the building's core. From NIST (2008).

around un-insulated central steel columns. The heated central columns lost their rigidity and began to sag, and trusses then transferred some of the weight above to the outer columns. In parallel, the heated floor structures began to sag, pulling inward on the buildings' exterior steel columns, which bowed inward and then buckled, initiating the buildings' collapse. [This is a somewhat oversimplified description of a complex situation; for full complexities, see the report NIST (2005).]

This column buckling was somewhat different from the buckling of a playing card, because of the inward pull of the sagging floors. Much more like our playing-card buckle was the fate of an adjacent, 47-story building called WTC7. When the towers collapsed, they injected burning debris onto and into WTC7. About seven hours later, fire-induced thermal expansion triggered a cascade of failures in floors 13–6, which left column number 79 with little stabilizing lateral support, so its effective length ℓ was increased far beyond $50r_g$. It then quickly buckled (Fig. 11.13a) in much the same manner as our playing card, followed by columns 80, then 81; then 77, 78, and 76 (NIST 2008, especially Sec. 2.4). Within seconds, the building's entire core was buckling (Fig. 11.13b).

11.6.3 Buckling with Lateral Force; Connection to Catastrophe Theory

Returning to the taller twin towers, we can crudely augment the inward pull of the sagging floors into our free-energy description of buckling, by adding a term $-F_{\text{lat}}\eta_0$ which represents the energy inserted into a bent column by a lateral force F_{lat} when its center has been displaced laterally through the distance η_0 . Then the free energy (11.57), made dimensionless

and with its terms rearranged, takes the form

$$\varphi \equiv \frac{V}{F_{\text{crit}}\ell} = \frac{1}{4} \left(\frac{\pi\eta_0}{2\ell} \right)^4 - \frac{1}{2} \left(\frac{2(F - F_{\text{crit}})}{F_{\text{crit}}} \right) \left(\frac{\pi\eta_0}{2\ell} \right)^2 - \left(\frac{2F_{\text{lat}}}{\pi F_{\text{crit}}} \right) \left(\frac{\pi\eta_0}{2\ell} \right). \quad (11.58)$$

Notice that this has the canonical form $\varphi = \frac{1}{4}b^4 - \frac{1}{2}xb^2 - yb$ for the potential that governs a *cuspl catastrophe*, whose state variable is $b = \pi\eta_0/2\ell$ and control variables are $x = 2(F - F_{\text{crit}})/F_{\text{crit}}$ and $y = 2F_{\text{lat}}/F_{\text{crit}}$; see Ex. 7.13b in Chap. 7.⁹ From the elementary mathematics of this catastrophe, as worked out in that exercise, we learn that: *although the lateral force F_{lat} will make the column bend, it will not induce a bifurcation of equilibria until the control-space cusp $y = \pm 2(x/3)^{3/2}$ is reached, i.e. until*

$$\frac{F_{\text{lat}}}{F_{\text{crit}}} = \pm \pi \left(\frac{F - F_{\text{crit}}}{2F_{\text{crit}}} \right)^{3/2}. \quad (11.59)$$

Notice that the lateral force F_{lat} actually *delays* the bifurcation to a higher vertical force, $F > F_{\text{crit}}$. However, this is not terribly important for the physical buckling, since the column in this case is bent from the outset, and as F_{lat} increases, it stops carrying its share of the building's weight and it moves smoothly toward its yield point and rupture; Ex. 11.16.

11.6.4 Other Bifurcations: Venus Fly Trap, Whirling Shaft, Triaxial Stars, Onset of Turbulence

This bifurcation of equilibria, associated with the buckling of a column, is just one of many bifurcations that occur in physical systems. Another is a buckling type bifurcation that occurs in the 2-dimensional leaves of the Venus Fly-Trap plant; the plant uses the associated instability to snap together a pair of leaves in a small fraction of a second, thereby capturing insects for it to swallow; see Fortere et. al. (2005). Yet another is the onset of a lateral bend in a shaft (rod) that spins around its longitudinal axis; see Sec. 286 of Love (1927). This is called *whirling*; it is an issue in drive shafts for automobiles and propellers, and a variant of it occurs in spinning DNA molecules during replication—see Wolgemuth, Powers and Goldstein (2000). One more example is the development of triaxiality in self-gravitating fluid masses (i.e. stars), when their rotational kinetic energy reaches a critical value, about 1/4 of their gravitational energy; see Chandrasekhar (1962). Bifurcations also play a major role in the onset of turbulence in fluids and in the route to chaos in other dynamical systems; we shall study this in Sec. 15.6.

For further details on the mathematics of bifurcations with emphasis on elastostatics and elastodynamics, see, e.g., Chap. 7 of Marsden and Hughes (1986). For details on buckling from an engineering viewpoint, see Chap. 11 of Ugural and Fenster (2012).

EXERCISES

⁹The lateral force F_{lat} makes the bifurcation *structurally stable*, in the language of catastrophe theory (discussed near the end of Sec. 7.5), and thereby makes it describable by one of the generic catastrophes. Without F_{lat} , the bifurcation is not structurally stable.

Exercise 11.14 *Derivation and Example: Bend as a Function of Applied Force*

Derive Eq. (11.56) relating the angle $\theta_o = (d\eta/dx)_{x=0} = k\eta_o = \pi\eta_o/\ell$ to the applied force F when the card has an $n = 1$, arched shape. Hint: Use the elastica differential equation $d^2\theta/dx^2 = -(F/D)\sin\theta$ [Eq. (11.50d)] for the angle between the card and the applied force at distance x from the card's end. The $\sin\theta$ becomes θ in the linear approximation used in the text; the nonlinearities embodied in the sine give rise to the desired relation. The following steps along the way toward a solution are mathematically the same as used when computing the period of a pendulum as a function of its amplitude of swing.

- (a) Derive the first integral of the elastica equation

$$(d\theta/dx)^2 = 2(F/D)(\cos\theta - \cos\theta_o), \quad (11.60)$$

where θ_o is an integration constant. Show that the boundary condition of no bending torque (no inflexion of the card's shape) at the card ends implies $\theta = \theta_o$ at $x = 0$ and $x = \ell$; whence $\theta = 0$ at the card's center, $x = \ell/2$.

- (b) Integrate the differential equation (11.60) to obtain

$$\frac{\ell}{2} = \sqrt{\frac{D}{2F}} \int_0^{\theta_o} \frac{d\theta}{\sqrt{\cos\theta - \cos\theta_o}}. \quad (11.61)$$

- (c) Perform the change of variable
- $\sin(\theta/2) = \sin(\theta_o/2)\sin\phi$
- and thereby bring Eq. (11.61) into the form

$$\ell = 2\sqrt{\frac{D}{F}} \int_0^{\pi/2} \frac{d\phi}{\sqrt{1 - \sin^2(\theta_o/2)\sin^2\phi}} = 2\sqrt{\frac{D}{F}} K[\sin^2(\theta_o/2)]. \quad (11.62)$$

Here $K(y)$ is the complete elliptic integral of the first type, with the parametrization used by Mathematica (which differs from many books).

- (d) Expand Eq. (11.62) in powers of
- $\sin^2(\theta_o/2)$
- to obtain

$$F = F_{\text{crit}} \frac{4}{\pi^2} K^2[\sin^2(\theta_o/2)] = F_{\text{crit}} \left[1 + \frac{1}{2} \sin^2(\theta_o/2) + \frac{11}{32} \sin^4(\theta_o/2) + \dots \right]. \quad (11.63)$$

Then expand this in powers of $\theta_o/2$ to obtain our desired result, Eq. (11.56).

Exercise 11.15 *Problem: Free Energy of a Bent, Compressed Beam*

Derive Eq. (11.57) for the free energy V of a beam that is compressed with a force F and has a critical compression $F_{\text{crit}} = \pi^2 D/\ell^2$, where D is its flexural rigidity. [Hint: It must be that $\partial V/\partial\eta_0 = 0$ gives Eq. (11.56) for the beam's equilibrium bend amplitude η_0 as a function of $F - F_{\text{crit}}$. Use this to reduce to reduce the number of terms in $V(\eta_0)$ in Eq. (11.57) that you need to derive.

Exercise 11.16 *Problem: Bent Beam with Lateral Force*

Explore, numerically, the free energy (11.58) of a bent beam with a compressive force F and lateral force F_{lat} . Examine how the extrema (equilibrium states) evolve as F and F_{lat} change, and deduce the physical consequences.

Exercise 11.17 ***Problem: Applications of Buckling — Mountains and Pipes*

Buckling plays a role in many natural and man-made phenomena. Explore the following examples:

- (a) **Mountain building.** When two continental plates are in (very slow) collision, the compressional force near their interface drives their crustal rock to buckle upward, producing mountains. Estimate how high such mountains can be on Earth and on Mars, and compare your estimates with their actual heights. Read about such mountain building in books or on the web.
- (b) **Thermal expansion of pipes.** When a segment of pipe is heated, e.g. by the rising sun in the morning, it will expand. If its ends are held fixed, this can easily produce a large enough longitudinal stress to buckle the pipe. How would you deal with this in an oil pipeline on the earth's surface? In a long vacuum tube? Compare your answers with standard engineering solutions, which you will find in books or on the web.

11.7 Reducing the Elastostatic Equations to Two Dimensions for a Deformed Thin Plate: Stress-Polishing a Telescope Mirror

The world's largest optical telescopes (as of 2013), the two ten meter Keck telescopes, are located on Mauna Kea in Hawaii. It is very difficult to support traditional, monolithic mirrors so that the mirror surfaces maintain their shape (their "figure") as the telescope slews, because they are so heavy; so for Keck a new method of fabrication was sought. The solution devised by Jerry Nelson and his colleagues was to construct the telescope out of 36 separate hexagons, each 0.9m on a side. However, this posed a second problem, grinding each hexagon's reflecting surface to the required hyperboloidal shape. For this, a novel technique called *stressed mirror polishing* was developed. This technique relies on the fact that it is relatively easy to grind a surface to a spherical shape, but technically highly challenging to create a non-axisymmetric shape. So, during the grinding, stresses are applied around the boundary of the mirror to deform it, and a spherical surface is produced. The stresses are then removed and the mirror springs into the desired nonspherical shape. Computing the necessary stresses is a problem in classical elasticity theory and, in fact, is a good example of a large number of applications where the elastic body can be approximated as a thin

plate and its shape can be analyzed using elasticity equations that are reduced from three dimensions to two by the method of moments.

For stress polishing of mirrors, the applied stresses are so large that we can ignore gravitational forces (at least in our simplified treatment). We suppose that the hexagonal mirror has a uniform thickness h and idealize it as a circle of radius R , and we introduce Cartesian coordinates with (x, y) in the horizontal plane (the plane of the mirror before deformation and polishing begin), and z vertical. The mirror is deformed as a result of a net vertical force per unit area (pressure) $P(x, y)$. This force is applied at the lower surface when positive and the upper surface when negative. In addition, there are shear forces and bending moments applied around the rim of the mirror.

As in our analysis of a cantilever in Sec. 11.5, we assume the existence of a neutral surface in the deformed mirror, where the horizontal strain vanishes, $T_{ab} = 0$. (*Here and below we use letters from the early part of the Latin alphabet for horizontal $x = x^1$, $y = x^2$ components.*) We denote the vertical displacement of the neutral surface by $\eta(x, y)$. By applying the method of moments to the three-dimensional equation stress balance equation $T_{jk,k} = 0$ in a manner similar to our cantilever analysis, we obtain the following two-dimensional equation for the mirror's shape:

$$\boxed{\nabla^2(\nabla^2\eta) = P(x, y)/D}. \quad (11.64a)$$

Here ∇^2 is the horizontal Laplacian, i.e. $\nabla^2\eta \equiv \eta_{,aa} = \eta_{,xx} + \eta_{,yy}$. Equation (11.64a) is the two-dimensional analog of the equation $d^4\eta/dx^4 = W(x)/D$ for the shape of a cantilever on which a downward force per unit length $W(x)$ acts [Eq. (11.46)]. The two-dimensional flexural rigidity that appears in Eq. (11.64a) is

$$\boxed{D = \frac{Eh^3}{12(1 - \nu^2)}}, \quad (11.64b)$$

where E is the mirror's Young's modulus, h is its thickness and ν is its Poisson's ratio. The quantity $\nabla^2\nabla^2$ that operates on η in the shape equation (11.64a) is called the *biharmonic operator*; it also appears in 3-dimensional form in the biharmonic equation (11.35a) for the displacement inside a homogeneous, isotropic body to which surface stresses are applied.

The shape equation (11.64a) must be solved subject to boundary conditions around the mirror's rim: the applied shear forces and bending torques.

The individual Keck mirror segments were constructed out of a ceramic material with Young's modulus $E = 89\text{GPa}$ and Poisson's ratio $\nu = 0.24$ (cf. Table 11.1). A mechanical jig was constructed to apply the shear forces and bending torques at 24 uniformly spaced points around the rim of the mirror (Figure 11.14). The maximum stress was applied for the six outermost mirrors and was $2.4 \times 10^6\text{N m}^{-2}$, 12 per cent of the breaking tensile strength ($2 \times 10^7\text{N m}^{-2}$).

This stress-polishing worked beautifully and the Keck telescopes have become highly successful tools for astronomical research.

EXERCISES

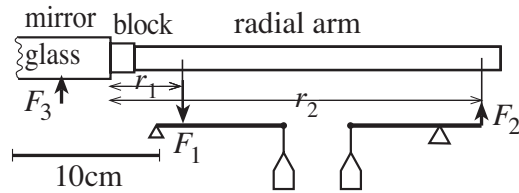


Fig. 11.14: Schematic showing the mirror rim, a radial arm attached to it via a block, and a lever assembly used to apply shear forces and bending torques to the rim during stress polishing. (F_1 need not equal F_2 as there is a pressure P applied to the back surface of the mirror and forces applied at 23 other points around its rim.) The shear force on the mirror rim is $S = F_2 - F_1$ and the bending torque is $M = r_2 F_2 - r_1 F_1$.

Exercise 11.18 *** *Derivation and Example: Dimensionally Reduced Shape Equation for a Stressed Plate*

Use the method of moments (Sec. 11.5) to derive the two-dimensional shape equation (11.64a) for the stress-induced deformation of a thin plate, and expression (11.64b) for the 2-dimensional flexural rigidity. Here is a step-by-step guide, in case you want or need it:

- (a) First show, on geometrical grounds, that the in-plane strain is related to the vertical displacement by [cf. Eq. (11.41a)]

$$\xi_{a,b} = -z\eta_{,ab} . \quad (11.65a)$$

- (b) Next derive an expression for the horizontal components of the stress, T_{ab} , in terms of double derivatives of the displacement function $\eta(x, y)$ [analog of $T_{xx} = -Ez d^2\eta/dx^2$, Eq. (11.41b), for a stressed rod]. This can be done (i) by arguing on physical grounds that the vertical component of stress, T_{zz} , is much smaller than the horizontal components and therefore can be approximated as zero [an approximation to be checked in part (f) below], (ii) by expressing $T_{zz} = 0$ in terms of the strain and thence displacement and using Eqs. (11.40) to arrive at

$$\Theta = - \left(\frac{1 - 2\nu}{1 - \nu} \right) z \nabla^2 \eta , \quad (11.65b)$$

where ∇^2 is the horizontal Laplacian, (iii) by then writing T_{ab} in terms of Θ and $\xi_{a,b}$ and combining with Eqs. (11.65a) and (11.65b) to get the desired equation:

$$T_{ab} = Ez \left[\frac{\nu}{(1 - \nu^2)} \nabla^2 \eta \delta_{ab} + \frac{\eta_{,ab}}{(1 + \nu)} \right] . \quad (11.65c)$$

- (c) With the aid of this equation, write the horizontal force density in the form

$$f_a = -T_{ab,b} - T_{az,z} = -\frac{Ez}{1 - \nu^2} \nabla^2 \eta_{,a} - T_{az,z} = 0 . \quad (11.65d)$$

Then, as in the cantilever analysis [Eq. (11.41d)], reduce the dimensionality of this force equation by the method of moments. The zero'th moment (integral over z) vanishes;

why? Therefore, the lowest nonvanishing moment is the first (multiply f_a by z and integrate). Show that this gives

$$S_a \equiv \int T_{za} dz = D \nabla^2 \eta_{,a} , \quad (11.65e)$$

where D is the 2-dimensional flexural rigidity (11.64b). The quantity S_a is the vertical shear force per unit length acting perpendicular to a line in the mirror, whose normal is in the direction a ; it is the 2-dimensional analog of a stressed rod's shear force S [Eq. (11.42a)].

- (d) For physical insight into Eq. (11.65e), define the bending torque per unit length (bending torque density)

$$M_{ab} \equiv \int z T_{ab} dz , \quad (11.65f)$$

and show with the aid of Eq. (11.65c) that (11.65e) is the law of torque balance $S_a = M_{ab,b}$ — the 2-dimensional analog of a stressed rod's $S = dM/dx$ [Eq. (11.43)].

- (e) Compute the total vertical shearing force acting on a small area of the plate as the line integral of S_a around its boundary, and by applying Gauss's theorem, deduce that the vertical shear force per unit area is $S_{a,a}$. Argue that this must be balanced by the net pressure P applied to the face of the plate, and thereby deduce the *law of vertical force balance*.

$$S_{a,a} = P . \quad (11.65g)$$

By combining with the law of torque balance (11.65e), obtain the plate's bending equation $\nabla^2(\nabla^2 \eta) = P/D$, Eq. (11.64a) — the final result we were seeking.

- (f) Use this bending equation to verify the approximation made in part (b), that T_{zz} is small compared to the horizontal stresses; specifically, show that $T_{zz} \simeq P$ is $O(h/R)^2 T_{ab}$, where h is the plate thickness and R is the plate radius.

Exercise 11.19 Example: Paraboloidal Mirror

Show how to construct a paraboloidal mirror of radius R and focal length f by stressed polishing.

- (a) Adopt a strategy of polishing the stressed mirror into a segment of a sphere with radius of curvature equal to that of the desired paraboloid at its center, $r = 0$. By comparing the shape of the desired paraboloid to that of the sphere, show that the required vertical displacement of the stressed mirror during polishing is

$$\eta(r) = \frac{r^4}{64f^3} ,$$

where r is the radial coordinate and we only retain terms of leading order.

(b) Hence use Eq. (11.64a) to show that a uniform force per unit area

$$P = \frac{D}{f^3},$$

where D is the Flexural Rigidity, must be applied to the bottom of the mirror. (Ignore the weight of the mirror.)

(c) Hence show that if there are N equally-spaced levers attached at the rim, the vertical force applied at each of them must be

$$F_z = \frac{\pi DR^2}{Nf^3},$$

and the associated bending torque is

$$M = \frac{\pi DR^3}{2Nf^3}.$$

(d) Show that the radial displacement inside the mirror is

$$\xi_r = -\frac{r^3 z}{16f^3},$$

where z is the vertical distance from the neutral surface, halfway through the mirror.

(e) Hence evaluate the expansion Θ and the components of the shear tensor Σ and show that the maximum stress in the mirror is

$$T_{\max} = \frac{(3 - 2\nu)R^2 h E}{32(1 - 2\nu)(1 + \nu)f^3},$$

where h is the mirror thickness. Comment on the limitations of this technique for making a thick, “fast” (i.e. $2R/f$ large) mirror.

11.8 T2 Cylindrical and Spherical Coordinates: Connection Coefficients and Components of the Gradient of the Displacement Vector

Thus far, in our discussion of elasticity, we have restricted ourselves to Cartesian coordinates. However, many problems in elasticity are most efficiently solved using cylindrical or spherical coordinates, so in this section we shall develop some mathematical tools for those coordinate systems. In doing so, we follow the vectorial conventions of standard texts on

electrodynamics and quantum mechanics (e.g., Jackson 1999, and Messiah 1962): We introduce an *orthonormal* set of basis vectors associated with each of our curvilinear coordinate systems; the coordinate lines are orthogonal to each other, and the basis vectors have unit lengths and point along the coordinate lines. In our study of continuum mechanics (Part IV – Elasticity, Part V – Fluid Mechanics, and Part VI – Plasma Physics), we shall follow this practice. Then in studying General Relativity and Cosmology (Part VII), we shall introduce and use basis vectors that are *not* orthonormal.

Our notation for cylindrical coordinates is (ϖ, ϕ, z) ; ϖ (pronounced “pomega”) is distance from the z axis, and ϕ is angle around the z axis, so

$$\varpi = \sqrt{x^2 + y^2}, \quad \phi = \arctan(y/x). \quad (11.66a)$$

The unit basis vectors that point along the coordinate axes are denoted \mathbf{e}_ϖ , \mathbf{e}_ϕ , \mathbf{e}_z , and are related to the Cartesian basis vectors by

$$\mathbf{e}_\varpi = (x/\varpi)\mathbf{e}_x + (y/\varpi)\mathbf{e}_y, \quad \mathbf{e}_\phi = -(y/\varpi)\mathbf{e}_x + (x/\varpi)\mathbf{e}_y, \quad \mathbf{e}_z = \text{Cartesian } \mathbf{e}_z. \quad (11.66b)$$

Our notation for spherical coordinates is (r, θ, ϕ) , with (as should be very familiar)

$$r = \sqrt{x^2 + y^2 + z^2}, \quad \theta = \arccos(z/r), \quad \phi = \arctan(y/x). \quad (11.67a)$$

The unit basis vectors associated with these coordinates are

$$\mathbf{e}_r = \frac{x}{r}\mathbf{e}_x + \frac{y}{r}\mathbf{e}_y + \frac{z}{r}\mathbf{e}_z, \quad \mathbf{e}_\theta = \frac{z}{r}\mathbf{e}_\varpi - \frac{\varpi}{r}\mathbf{e}_z, \quad \mathbf{e}_\phi = -\frac{y}{\varpi}\mathbf{e}_x + \frac{x}{\varpi}\mathbf{e}_y. \quad (11.67b)$$

Because our bases are orthonormal, the components of the metric of 3-dimensional space retain the Kronecker-delta values

$$\boxed{g_{jk} \equiv \mathbf{e}_j \cdot \mathbf{e}_k = \delta_{jk}}, \quad (11.68)$$

which permits us to keep all vector and tensor indices down, by contrast with spacetime where we must distinguish between up and down; cf. Sec. 2.5.¹⁰

In Jackson (1999), Messiah (1962) and other standard texts, formulas are written down for the gradient and Laplacian of a scalar field, and the divergence and curl of a vector field, in cylindrical and spherical coordinates; and one uses these formulas over and over again. In elasticity theory, we deal largely with second rank tensors, and will need formulae for their various derivatives in cylindrical and spherical coordinates. In this book we introduce a mathematical tool, *connection coefficients* Γ_{ijk} , by which those formulae can be derived when needed.

The connection coefficients quantify the turning of the orthonormal basis vectors as one moves from point to point in Euclidean 3-space; i.e., they tell us how the basis vectors at one point in space are *connected to* (related to) those at another point. More specifically, we define Γ_{ijk} by the two equivalent relations

$$\boxed{\nabla_k \mathbf{e}_j = \Gamma_{ijk} \mathbf{e}_i; \quad \Gamma_{ijk} = \mathbf{e}_i \cdot (\nabla_k \mathbf{e}_j)}. \quad (11.69)$$

¹⁰Occasionally, e.g. in the useful equation $\epsilon_{ijm}\epsilon_{klm} = \delta_{kl}^{ij} \equiv \delta_k^i \delta_l^j - \delta_l^i \delta_k^j$ [Eq. (1.23)], it is convenient to put some indices up. In our orthonormal basis, any component with an index up is equal to that same component with an index down; e.g., $\delta_k^i \equiv \delta_{ik}$.

Here $\nabla_k \equiv \nabla_{\mathbf{e}_k}$ is the directional derivative along the orthonormal basis vector \mathbf{e}_k ; cf. Eq. (1.15a). Notice that (as is true quite generally; cf. Sec. 1.7) the differentiation index comes *last* on Γ ; and notice that the middle index of Γ names the basis vector that is differentiated. Because our basis is orthonormal, it must be that $\nabla_k(\mathbf{e}_i \cdot \mathbf{e}_j) = 0$. Expanding this out using the standard rule for differentiating products, we obtain $\mathbf{e}_j \cdot (\nabla_k \mathbf{e}_i) + \mathbf{e}_i \cdot (\nabla_k \mathbf{e}_j) = 0$. Then invoking the definition (11.69) of the connection coefficients, we see that Γ_{ijk} is antisymmetric on its first two indices:

$$\boxed{\Gamma_{ijk} = -\Gamma_{jik}}. \quad (11.70)$$

In Part VII, when we use non-orthonormal bases, this antisymmetry will break down.

It is straightforward to compute the connection coefficients for cylindrical and spherical coordinates from (i) the definition (11.69), (ii) expressions (11.66b) and (11.67b) for the cylindrical and spherical basis vectors in terms of the Cartesian basis vectors, and (iii) the fact that *in Cartesian coordinates the connection coefficients vanish* (\mathbf{e}_x , \mathbf{e}_y and \mathbf{e}_z do not rotate as one moves through Euclidean 3-space). One can also deduce the cylindrical and spherical connection coefficients by drawing pictures of the basis vectors and observing how they change from point to point. As an example, for cylindrical coordinates we see from Fig. 11.15 that $\nabla_\phi \mathbf{e}_\varpi = \mathbf{e}_\phi / \varpi$. A similar pictorial calculation (which the reader is encouraged to do) reveals that $\nabla_\phi \mathbf{e}_\phi = -\mathbf{e}_\varpi / \varpi$. All other derivatives vanish. By comparing with Eq. (11.69), we see that *the only nonzero connection coefficients in cylindrical coordinates are*

$$\boxed{\Gamma_{\varpi\phi\phi} = -\frac{1}{\varpi}, \quad \Gamma_{\phi\varpi\phi} = \frac{1}{\varpi}}, \quad (11.71)$$

which have the required antisymmetry [Eq. (11.70)]. Likewise, for spherical coordinates (Ex.

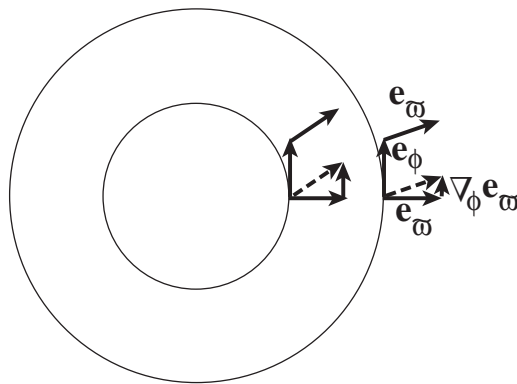


Fig. 11.15: Pictorial evaluation of $\Gamma_{\phi\varpi\phi}$. In the right-most assemblage of vectors we compute $\nabla_\phi \mathbf{e}_\varpi$ as follows: We draw the vector to be differentiated, \mathbf{e}_ϖ , at the tail of \mathbf{e}_ϕ (the vector along which we differentiate) and also at its head. We then subtract \mathbf{e}_ϖ at the head from that at the tail; this difference is $\nabla_\phi \mathbf{e}_\varpi$. It obviously points in the \mathbf{e}_ϕ direction. When we perform the same calculation at a radius ϖ that is smaller by a factor 2 (left assemblage of vectors), we obtain a result, $\nabla_\phi \mathbf{e}_\varpi$, that is twice as large. Therefore the length of this vector must scale as $1/\varpi$. By looking quantitatively at the length at some chosen radius ϖ , one can see that the multiplicative coefficient is unity: $\nabla_\phi \mathbf{e}_\varpi = \frac{1}{\varpi} \mathbf{e}_\phi$. Comparing with Eq. (11.69), we deduce that $\Gamma_{\phi\varpi\phi} = 1/\varpi$.

11.21)

$$\boxed{\Gamma_{\theta r\theta} = \Gamma_{\phi r\phi} = -\Gamma_{r\theta\theta} = -\Gamma_{r\phi\phi} = \frac{1}{r}, \quad \Gamma_{\phi\theta\phi} = -\Gamma_{\theta\phi\phi} = \frac{\cot\theta}{r}}; \quad (11.72)$$

These connection coefficients are the keys to differentiating vectors and tensors. Consider the gradient of the displacement, $\mathbf{w} = \nabla \boldsymbol{\xi}$. Applying the product rule for differentiation, we obtain

$$\nabla_k(\xi_j \mathbf{e}_j) = (\nabla_k \xi_j) \mathbf{e}_j + \xi_j (\nabla_k \mathbf{e}_j) = \xi_{j,k} \mathbf{e}_j + \xi_j \Gamma_{ljk} \mathbf{e}_l. \quad (11.73)$$

Here the comma denotes the directional derivative, along a basis vector, of the components treated as scalar fields. For example, *in cylindrical coordinates* we have

$$\xi_{i,\varpi} = \frac{\partial \xi_i}{\partial \varpi}, \quad \xi_{i,\phi} = \frac{1}{\varpi} \frac{\partial \xi_i}{\partial \phi}, \quad \xi_{i,z} = \frac{\partial \xi_i}{\partial z}; \quad (11.74)$$

and *in spherical coordinates* we have

$$\xi_{i,r} = \frac{\partial \xi_i}{\partial r}, \quad \xi_{i,\theta} = \frac{1}{r} \frac{\partial \xi_i}{\partial \theta}, \quad \xi_{i,\phi} = \frac{1}{r \sin \theta} \frac{\partial \xi_i}{\partial \phi}. \quad (11.75)$$

Taking the i 'th component of Eq. (11.73) we obtain

$$\boxed{W_{ik} = \xi_{i;k} = \xi_{i,k} + \Gamma_{ijk} \xi_j}. \quad (11.76)$$

Here $\xi_{i;k}$ are the nine components of the gradient of the vector field $\boldsymbol{\xi}(\mathbf{x})$.

We can use Eq. (11.76) to evaluate the expansion $\Theta = \text{Tr} \mathbf{W} = \nabla \cdot \boldsymbol{\xi}$. Using Eqs. (11.71) and (11.72), we obtain

$$\begin{aligned} \Theta = \nabla \cdot \boldsymbol{\xi} &= \frac{\partial \xi_\varpi}{\partial \varpi} + \frac{1}{\varpi} \frac{\partial \xi_\phi}{\partial \phi} + \frac{\partial \xi_z}{\partial z} + \frac{\xi_\varpi}{\varpi} \\ &= \frac{1}{\varpi} \frac{\partial}{\partial \varpi} (\varpi \xi_\varpi) + \frac{1}{\varpi} \frac{\partial \xi_\phi}{\partial \phi} + \frac{\partial \xi_z}{\partial z} \end{aligned} \quad (11.77)$$

in cylindrical coordinates, and

$$\begin{aligned} \Theta = \nabla \cdot \boldsymbol{\xi} &= \frac{\partial \xi_r}{\partial r} + \frac{1}{r} \frac{\partial \xi_\theta}{\partial \theta} + \frac{1}{r \sin \theta} \frac{\partial \xi_\phi}{\partial \phi} + \frac{2\xi_r}{r} + \frac{\cot \theta \xi_\theta}{r} \\ &= \frac{1}{r^2} \frac{\partial}{\partial r} (r^2 \xi_r) + \frac{1}{r \sin \theta} \frac{\partial}{\partial \theta} (\sin \theta \xi_\theta) + \frac{1}{r \sin \theta} \frac{\partial \xi_\phi}{\partial \phi} \end{aligned} \quad (11.78)$$

in spherical coordinates, in agreement with formulae in standard textbooks such as the flyleaf of Jackson (1999).

The components of the rotation are most easily deduced using $R_{ij} = -\epsilon_{ijk} \phi_k$ with $\boldsymbol{\phi} = \frac{1}{2} \nabla \times \boldsymbol{\xi}$, and the standard expressions for the curl in cylindrical and spherical coordinates (e.g., Jackson 1999). Since the rotation does not enter into elasticity theory in a significant way, we shall refrain from writing down the results. The components of the shear are computed in Box 11.4.

Box 11.4

T2 Shear Tensor in Spherical and Cylindrical Coordinates

Using our rules (11.76) for forming the gradient of a vector we can derive a general expression for the shear tensor

$$\begin{aligned}\Sigma_{ij} &= \frac{1}{2}(\xi_{i;j} + \xi_{j;i}) - \frac{1}{3}\delta_{ij}\xi_{k;k} \\ &= \frac{1}{2}(\xi_{i,j} + \xi_{j,i} + \Gamma_{ilj}\xi_l + \Gamma_{jli}\xi_l) - \frac{1}{3}\delta_{ij}(\xi_{k,k} + \Gamma_{klk}\xi_l) .\end{aligned}\quad (1)$$

Evaluating this *in cylindrical coordinates* using the connection coefficients (11.71), we obtain

$$\begin{aligned}\Sigma_{\varpi\varpi} &= \frac{2}{3}\frac{\partial\xi_{\varpi}}{\partial\varpi} - \frac{1}{3}\frac{\xi_{\varpi}}{\varpi} - \frac{1}{3\varpi}\frac{\partial\xi_{\phi}}{\partial\phi} - \frac{1}{3}\frac{\partial\xi_z}{\partial z} , \\ \Sigma_{\phi\phi} &= \frac{2}{3\varpi}\frac{\partial\xi_{\phi}}{\partial\phi} + \frac{2}{3}\frac{\xi_{\varpi}}{\varpi} - \frac{1}{3}\frac{\partial\xi_{\varpi}}{\partial\varpi} - \frac{1}{3}\frac{\partial\xi_z}{\partial z} , \\ \Sigma_{zz} &= \frac{2}{3}\frac{\partial\xi_z}{\partial z} - \frac{1}{3}\frac{\partial\xi_{\varpi}}{\partial\varpi} - \frac{1}{3}\frac{\xi_{\varpi}}{\varpi} - \frac{1}{3\varpi}\frac{\partial\xi_{\phi}}{\partial\phi} , \\ \Sigma_{\phi z} &= \Sigma_{z\phi} = \frac{1}{2\varpi}\frac{\partial\xi_z}{\partial\phi} + \frac{1}{2}\frac{\partial\xi_{\phi}}{\partial z} , \\ \Sigma_{z\varpi} &= \Sigma_{\varpi z} = \frac{1}{2}\frac{\partial\xi_{\varpi}}{\partial z} + \frac{1}{2}\frac{\partial\xi_z}{\partial\varpi} , \\ \Sigma_{\varpi\phi} &= \Sigma_{\phi\varpi} = \frac{1}{2}\frac{\partial\xi_{\phi}}{\partial\varpi} - \frac{\xi_{\phi}}{2\varpi} + \frac{1}{2\varpi}\frac{\partial\xi_{\varpi}}{\partial\phi} .\end{aligned}\quad (2)$$

Likewise, *in spherical coordinates* using the connection coefficients (11.72), we obtain

$$\begin{aligned}\Sigma_{rr} &= \frac{2}{3}\frac{\partial\xi_r}{\partial r} - \frac{2}{3r}\xi_r - \frac{\cot\theta}{3r}\xi_{\theta} - \frac{1}{3r}\frac{\partial\xi_{\theta}}{\partial\theta} - \frac{1}{3r\sin\theta}\frac{\partial\xi_{\phi}}{\partial\phi} , \\ \Sigma_{\theta\theta} &= \frac{2}{3r}\frac{\partial\xi_{\theta}}{\partial\theta} + \frac{\xi_r}{3r} - \frac{1}{3}\frac{\partial\xi_r}{\partial r} - \frac{\cot\theta\xi_{\theta}}{3r} - \frac{1}{3r\sin\theta}\frac{\partial\xi_{\phi}}{\partial\phi} , \\ \Sigma_{\phi\phi} &= \frac{2}{3r\sin\theta}\frac{\partial\xi_{\phi}}{\partial\phi} + \frac{2\cot\theta\xi_{\theta}}{3r} + \frac{\xi_r}{3r} - \frac{1}{3}\frac{\partial\xi_r}{\partial r} - \frac{1}{3r}\frac{\partial\xi_{\theta}}{\partial\theta} , \\ \Sigma_{\theta\phi} &= \Sigma_{\phi\theta} = \frac{1}{2r}\frac{\partial\xi_{\phi}}{\partial\theta} - \frac{\cot\theta\xi_{\phi}}{2r} + \frac{1}{2r\sin\theta}\frac{\partial\xi_{\theta}}{\partial\phi} , \\ \Sigma_{\phi r} &= \Sigma_{r\phi} = \frac{1}{2r\sin\theta}\frac{\partial\xi_r}{\partial\phi} + \frac{1}{2}\frac{\partial\xi_{\phi}}{\partial r} - \frac{\xi_{\phi}}{2r} , \\ \Sigma_{r\theta} &= \Sigma_{\theta r} = \frac{1}{2}\frac{\partial\xi_{\theta}}{\partial r} - \frac{\xi_{\theta}}{2r} + \frac{1}{2r}\frac{\partial\xi_r}{\partial\theta} .\end{aligned}\quad (3)$$

By a computation analogous to Eq. (11.73), we can construct an expression for the gradient of a tensor of any rank. For a second rank tensor $\mathbf{T} = T_{ij}\mathbf{e}_i \otimes \mathbf{e}_j$ we obtain (Ex. 11.20)

$$\boxed{T_{ij;k} = T_{ij,k} + \Gamma_{ilk}T_{lj} + \Gamma_{jlk}T_{il}}. \quad (11.79)$$

Equation (11.79) for the components of the gradient can be understood as follows: In cylindrical or spherical coordinates, the components T_{ij} can change from point to point as a result of two things: a change of the tensor \mathbf{T} , or the turning of the basis vectors. The two connection coefficient terms in Eq. (11.79) remove the effects of the basis turning, leaving in $T_{ij;k}$ only the influence of the change of \mathbf{T} itself. There are two correction terms corresponding to the two slots (indices) of \mathbf{T} ; the effects of basis turning on each slot get corrected one after another. If \mathbf{T} had had n slots, then there would have been n correction terms, each with the form of the two in Eq. (11.79).

These expressions for derivatives of tensors are not required to deal with the vector fields of introductory electromagnetic theory or quantum theory, but they are essential to manipulate the tensor fields encountered in elasticity. As we shall see in Sec. 24.3, with one further generalization, we can go on to differentiate tensors in any basis (orthonormal or non-orthonormal) in a curved spacetime, as is needed to perform calculations in general relativity.

Although the algebra of evaluating the components of derivatives such as (11.79) in explicit form (e.g., in terms of $\{r, \theta, \phi\}$) can be long and tedious when done by hand, in the modern era of symbolic manipulation via computers (e.g. Mathematica or Maple), the algebra can be done quickly and accurately to obtain expressions such as Eqs. (3) of Box 11.4.

EXERCISES

Exercise 11.20 *Derivation and Practice: Gradient of a Second Rank Tensor*

By a computation analogous to Eq. (11.73), derive Eq. (11.79) for the components of the gradient of a second rank tensor in any orthonormal basis

Exercise 11.21 *Derivation and Practice: Connection in Spherical Coordinates*

(a) By drawing pictures analogous to Fig. 11.15, show that

$$\nabla_{\phi}\mathbf{e}_r = \frac{1}{r}\mathbf{e}_{\phi}, \quad \nabla_{\theta}\mathbf{e}_r = \frac{1}{r}\mathbf{e}_{\theta}, \quad \nabla_{\phi}\mathbf{e}_{\theta} = \frac{\cot\theta}{r}\mathbf{e}_{\phi}. \quad (11.80)$$

(b) From these relations and antisymmetry on the first two indices [Eq. (11.70)], deduce the connection coefficients (11.72).

Exercise 11.22 *Derivation and Practice: Expansion in Cylindrical and Spherical Coordinates*

Derive Eqs. (11.77) and (11.78) for the divergence of the vector field $\boldsymbol{\xi}$ in cylindrical and spherical coordinates using the connection coefficients (11.71) and (11.72).

11.9 [T2] Solving the 3-Dimensional Navier-Cauchy Equation in Cylindrical Coordinates

11.9.1 [T2] Simple Methods: Pipe Fracture and Torsion Pendulum

As an example of an elastostatic problem with cylindrical symmetry, consider a cylindrical pipe that carries a high-pressure fluid (water, oil, natural gas, ...); Fig. 11.16. How thick must the pipe's wall be to ensure that it will not burst due to the fluid's pressure? We shall sketch the solution, leaving the details to the reader in Ex. 11.23.

We suppose, for simplicity, that the pipe's length is held fixed by its support system: it does not lengthen or shorten when the fluid pressure is changed. Then by symmetry, the displacement field in the pipe wall is purely radial and depends only on radius; i.e., its only nonzero component is $\xi_{\varpi}(\varpi)$. The radial dependence is governed by radial force balance,

$$f_{\varpi} = K\Theta_{;\varpi} + 2\mu\Sigma_{\varpi j;j} = 0. \quad (11.81)$$

[Eq. (11.31)].

Because ξ_{ϖ} is independent of ϕ and z , the expansion [Eq. (11.77)] is given by

$$\Theta = \frac{\partial \xi_{\varpi}}{\partial \varpi} + \frac{\xi_{\varpi}}{\varpi}. \quad (11.82)$$

The second term in the radial force balance equation (11.81) is proportional to $\Sigma_{\varpi j;j}$ which, using Eq. (11.79) and noting that the only nonzero connection coefficients are $\Gamma_{\varpi\phi\phi} = -\Gamma_{\phi\varpi\phi} = -1/\varpi$ [Eq. (11.71)] and that symmetry requires the shear tensor to be diagonal, becomes

$$\Sigma_{\varpi j;j} = \Sigma_{\varpi\varpi,\varpi} + \Gamma_{\varpi\phi\phi}\Sigma_{\phi\phi} + \Gamma_{\phi\varpi\phi}\Sigma_{\varpi\varpi}. \quad (11.83)$$

Inserting the components of the shear tensor from Eq. (2) of Box 11.4 and the values of the connection coefficients and comparing the result with Expression (11.82) for the expansion, we obtain the remarkable result that $\Sigma_{\varpi j;j} = \frac{2}{3}\partial\Theta/\partial\varpi$. Inserting this into the radial force

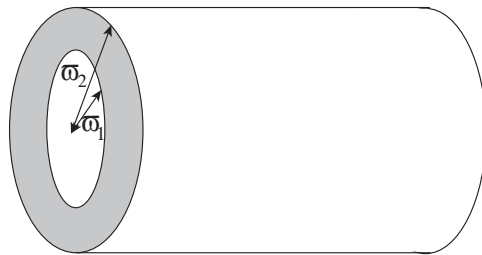


Fig. 11.16: A pipe whose wall has inner and outer radii ϖ_1 and ϖ_2 .

balance equation (11.81), we obtain

$$f_{\varpi} = \left(K + \frac{4\mu}{3} \right) \frac{\partial \Theta}{\partial \varpi} = 0. \quad (11.84)$$

Thus, *inside the pipe wall, the expansion is independent of radius ϖ* , and correspondingly, the radial displacement must have the form [cf. Eq. (11.82)]

$$\xi_{\varpi} = A\varpi + \frac{B}{\varpi} \quad (11.85)$$

for some constants A and B , whence $\Theta = 2A$ and $\Sigma_{\varpi\varpi} = \frac{1}{3}A - B/\varpi^2$. The values of A and B are fixed by the boundary conditions at the inner and outer faces of the pipe wall: $T_{\varpi\varpi} = P$ at $\varpi = \varpi_1$ (inner wall) and $T_{\varpi\varpi} = 0$ at $\varpi = \varpi_2$ (outer wall). Here P is the pressure of the fluid that the pipe carries and we have neglected the atmosphere's pressure on the outer face by comparison. Evaluating $T_{\varpi\varpi} = -K\Theta - 2\mu\Sigma_{\varpi\varpi}$ and then imposing these boundary conditions, we obtain

$$A = \frac{P}{2(K + \mu/3)} \frac{\varpi_1^2}{\varpi_2^2 - \varpi_1^2}, \quad B = \frac{P}{2\mu} \frac{\varpi_1^2 \varpi_2^2}{\varpi_2^2 - \varpi_1^2}. \quad (11.86)$$

The only nonvanishing components of the strain then work out to be

$$S_{\varpi\varpi} = \frac{\partial \xi_{\varpi}}{\partial \varpi} = A - \frac{B}{\varpi^2}, \quad S_{\phi\phi} = \frac{\xi_{\varpi}}{\varpi} = A + \frac{B}{\varpi^2}. \quad (11.87)$$

This strain is maximal at the inner wall of the pipe; expressing it in terms of the ratio $\zeta \equiv \varpi_2/\varpi_1$ of the outer to the inner pipe radius and using the values of $K = 180$ GPa and $\mu = 81$ GPa for steel, we bring this maximum strain into the form

$$S_{\varpi\varpi} \simeq -\frac{P}{\mu} \frac{5\zeta^2 - 2}{10(\zeta^2 - 1)}, \quad S_{\phi\phi} \simeq \frac{P}{\mu} \frac{5\zeta^2 + 2}{10(\zeta^2 - 1)}. \quad (11.88)$$

Note that $|S_{\phi\phi}| > |S_{\varpi\varpi}|$.

The pipe will break at a strain $\sim 10^{-3}$; for safety it is best to keep the actual strain smaller than this by an order of magnitude, $|S_{ij}| \lesssim 10^{-4}$. A typical pressure for an oil pipeline is $P \simeq 10$ atmospheres $\simeq 10^6$ Pa, compared to the shear modulus of steel $\mu = 81$ GPa, so $P/\mu \simeq 1.2 \times 10^{-5}$. Inserting this into Eq. (11.88) with $|S_{\phi\phi}| \lesssim 10^{-4}$, we deduce that the ratio of the pipe's outer radius to its inner radius must be $\zeta = \varpi_2/\varpi_1 \gtrsim 1.04$. If the pipe has a diameter of a half meter, then its wall thickness should be about one centimeter or more. This is typical of the pipes in oil pipelines.

Exercise 11.24 presents a second fairly simple example of elastostatics in cylindrical coordinates: a computation of the period of a torsion pendulum.

EXERCISES

Exercise 11.23 *Derivation and Practice: Fracture of a Pipe*

Fill in the details of the text's analysis of the deformation of a pipe carrying a high-pressure fluid, and the wall thickness required to protect the pipe against fracture, Sec. 11.9.1.

Exercise 11.24 *Practice: Torsion pendulum*

A torsion pendulum is a very useful tool for testing the equivalence principle, for seeking evidence for hypothetical *fifth* (not to mention *sixth*) forces, and for searching for deviations from gravity's inverse square law on submillimeter scales, which could arise from gravity feeling macroscopic higher spatial dimensions. (See, e.g., Kapner et. al. 2008, and Wagner et. al. 2013). It would be advantageous to design a torsion pendulum with a one day period (Figure 11.17). In this exercise we shall estimate whether this is possible. The pendulum consists of a thin cylindrical wire of length l and radius a . At the bottom of the wire are suspended three masses at the corners of an equilateral triangle at a distance b from the wire.

- (a) Show that the longitudinal strain is

$$\xi_{z;z} = \frac{3mg}{\pi a^2 E} . \quad (11.89a)$$

- (b) What component of shear is responsible for the restoring force in the wire, which causes torsion pendulum to oscillate?
- (c) Show that the pendulum undergoes torsional oscillations with period

$$P = 2\pi \left(\frac{\ell}{g} \right)^{1/2} \left(\frac{2b^2 E \xi_{z;z}}{a^2 \mu} \right)^{1/2} . \quad (11.89b)$$

- (d) Do you think you could design a pendulum that attains the goal of a one day period?

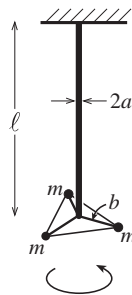


Fig. 11.17: Torsion Pendulum in Ex. 11.24.

11.9.2 **T2** Separation of Variables and Green's Functions: Thermoelastic Noise in Mirrors

In more complicated situations that have moderate amounts of symmetry, the elastostatic equations can be solved by the same kinds of sophisticated mathematical techniques as one uses in electrostatics: separation of variables, Green's functions, complex potentials, or integral transform methods; see, e.g. Gladwell (1980). We provide an example in this section, focusing on separation of variables and Green's functions.

Motivation

Our example is motivated by an important issue in high-precision measurements with light, including, among others, gravitational-wave detectors and quantum optics experiments in which photons and atoms are put into entangled nonclassical states by coupling them to each other inside Fabry Perot cavities.

In these situations, noise due to thermal motions of the mirror faces, is a serious issue. It can hide a gravitational wave, and it can cause decoherence of the atom/photon quantum states. In Sec. 6.8.2, we formulated a generalized fluctuation-dissipation theorem by which this mirror thermal noise can be computed (Levin 1998):

In a thought experiment, one applies to the mirror face a force F_o that oscillates at some frequency f at which one wants to evaluate the thermal noise, and that has the same transverse pressure distribution as the light beam — say, for concreteness, a Gaussian distribution:

$$T_{zz}^{\text{applied}} = \frac{e^{-\varpi^2/\varpi_o^2}}{\pi\varpi_o^2} F_o \cos(2\pi ft) . \quad (11.90)$$

This applied pressure induces a strain distribution \mathbf{S} inside the mirror, and that oscillating strain interacts with imperfections to dissipate energy at some rate $W_{\text{diss}}(f)$. The fluctuation-dissipation theorem says that in the real experiment, where the light beam bounces off the mirror, the reflected light will encode a noisy transverse-averaged position q for the mirror face, and the noise spectral density for q will be

$$S_q(f) = \frac{8W_{\text{diss}}(f)k_B T}{F_o^2} \quad (11.91)$$

[Eq. (6.88b)].

Now, even if one could make the mirror perfect (no dislocations or impurities), so there is no dissipation due to imperfections, there will remain one other source of dissipation in this thought experiment: The applied pressure (11.90) will produce a spatially inhomogeneous expansion $\Theta(\mathbf{x}, t)$ inside the mirror, which in turn will produce the thermoelastic temperature change $\Delta T/T = -(3\alpha K/\rho c_V)\Theta$ [Eq. (11.30)]. The gradient of this temperature will induce heat to flow, with a thermal energy flux $\mathbf{F}_{\text{th}} = -\kappa\nabla\Delta T$, where κ is the thermal conductivity. When an amount Q of this thermal energy flows from a region with temperature T to a region of lower temperature $T - dT$, it produces an entropy increase $dS = Q/(T - dT) - Q/T = QdT/T^2$; and correspondingly, there is a rate of entropy increase per unit volume given by $dS/dV dt = -\mathbf{F}_{\text{th}} \cdot \nabla\Delta T/T^2 = \kappa(\nabla\Delta T)^2/T^2$. This entropy increase has an accompanying

energy dissipation rate $W_{\text{diss}} = \int T(dS/dtdV)dv = \int \kappa(\nabla\Delta T)^2 T dV$. Expressing ΔT in terms of the expansion that drives it via $\Delta T/T = -(3\alpha K/\rho c_V)\Theta$, and inserting that into Eq. (11.91), we obtain the thermal noise spectral density that the experimenters must contend with:

$$S_q(f) = \frac{2\kappa E^2 \alpha^2 k T^2}{(1-2\nu)^2 c_V^2 \rho^2 F_o^2 (2\pi f)^2} \left\langle \int (\nabla\Theta)^2 \varpi d\phi d\varpi dz \right\rangle. \quad (11.92)$$

Because the dissipation producing this noise is due to heat flowing down a thermoelastic temperature gradient, it is called *thermoelastic noise*.

This is the motivation for our elasticity problem: To evaluate this thermoelastic noise, *we must compute the expansion $\Theta(\mathbf{x}, t)$ inside a mirror, produced by the oscillating pressure (11.90) on the mirror face*; and we must then perform the integral (11.92).

Solution for Θ via separation of variables

The frequencies f at which we wish to evaluate the thermal noise are very low compared to the sound travel time across the mirror, so in computing Θ we can regard the force as oscillating very slowly; i.e., we can use our elastostatic equations rather than dynamical equations of the next chapter. Also, the size of the light spot on the mirror is usually small compared to the mirror's transverse size and thickness, so we shall idealize the mirror as being infinitely large and thick—a homogeneous “half space” of isotropic, elastic material.

Because the applied stress is axially symmetric, the induced strain and expansion will also be axially symmetric, and are thus computed most easily using cylindrical coordinates. Our challenge, then, is to solve the Navier-Cauchy equation $\mathbf{f} = (K + \frac{1}{3}\mu)\nabla(\nabla \cdot \boldsymbol{\xi}) + \mu\nabla^2\boldsymbol{\xi} = 0$ for the cylindrical components $\xi_\varpi(z, \varpi)$ and $\xi_z(z, \varpi)$ of the displacement, and then evaluate the divergence $\Theta = \nabla \cdot \boldsymbol{\xi}$. (The component ξ_ϕ vanishes by symmetry.)

Equations of elasticity in cylindrical coordinates, and their homogeneous solution

It is straightforward, using the techniques of Sec. 11.8, to compute the cylindrical components of \mathbf{f} . Reexpressing the bulk and shear moduli K and μ in terms of Young's modulus E and Poisson's ratio ν [Eq. (11.40)] and setting the internal forces to zero, we obtain

$$f_\varpi = \frac{E}{2(1+\nu)(1-2\nu)} \left[2(1-\nu) \left(\frac{\partial^2 \xi_\varpi}{\partial \varpi^2} + \frac{1}{\varpi} \frac{\partial \xi_\varpi}{\partial \varpi} - \frac{\xi_\varpi}{\varpi^2} \right) + (1-2\nu) \frac{\partial^2 \xi_\varpi}{\partial z^2} + \frac{\partial^2 \xi_z}{\partial z \partial \varpi} \right] = 0, \quad (11.93a)$$

$$f_z = \frac{E}{2(1+\nu)(1-2\nu)} \left[(1-2\nu) \left(\frac{\partial^2 \xi_z}{\partial \varpi^2} + \frac{1}{\varpi} \frac{\partial \xi_z}{\partial \varpi} \right) + 2(1-\nu) \frac{\partial^2 \xi_z}{\partial z^2} + \frac{\partial^2 \xi_\varpi}{\partial z \partial \varpi} + \frac{1}{\varpi} \frac{\partial \xi_\varpi}{\partial z} \right] = 0. \quad (11.93b)$$

These are two coupled, linear, second-order differential equations for the two unknown components of the displacement vector. As with the analogous equations of electrostatics and magnetostatics, these can be solved by separation of variables, i.e. by setting $\xi_\varpi = R_\varpi(\varpi)Z_\varpi(z)$ and $\xi_z = R_z(\varpi)Z_z(z)$, and inserting into Eq. (11.93a). We seek the general

solution that dies out at large ϖ and z . The general solution of this sort, to the complicated looking Eqs. (11.93), turns out to be (really!!)

$$\begin{aligned}\xi_{\varpi} &= \int_0^{\infty} [\alpha(k) - (2 - 2\nu - kz)\beta(k)] e^{-kz} J_1(k\varpi) k dk , \\ \xi_z &= \int_0^{\infty} [\alpha(k) + (1 - 2\nu + kz)\beta(k)] e^{-kz} J_0(k\varpi) dk .\end{aligned}\quad (11.94)$$

Here J_0 and J_1 are Bessel functions of order 0 and 1, and $\alpha(k)$ and $\beta(k)$ are arbitrary functions.

Boundary Conditions

The functions $\alpha(k)$ and $\beta(k)$ are determined by boundary conditions on the face of the test mass: The force per unit area exerted across the face by the strained test-mass material, T_{zj} at $z = 0$ with $j = \{\varpi, \phi, z\}$, must be balanced by the applied force per unit area, T_{zj}^{applied} [Eq. (11.90)]. The (shear) forces in the ϕ direction, $T_{z\phi}$ and $T_{z\phi}^{\text{applied}}$, vanish because of cylindrical symmetry and thus provide no useful boundary condition. The (shear) force in the ϖ direction, which must vanish since $T_{z\varpi}^{\text{applied}} = 0$, is given by [cf. Eq. (2) in Box 11.4]

$$T_{z\varpi}(z = 0) = -2\mu\Sigma_{z\varpi} = -\mu \left(\frac{\partial \xi_z}{\partial \varpi} + \frac{\partial \xi_{\varpi}}{\partial z} \right) = -\mu \int_0^{\infty} [\beta(k) - \alpha(k)] J_1(kz) k dk = 0 ,\quad (11.95)$$

which implies that $\beta(k) = \alpha(k)$. The (normal) force in the z direction, which must balance the applied pressure (11.90), is $T_{zz} = -K\Theta - 2\mu\Sigma_{zz}$; using Eq. (2) in Box 11.4 and Eqs. (11.94) and (11.90), this reduces to

$$T_{zz}(z = 0) = -2\mu \int_0^{\infty} \alpha(k) J_0(k\varpi) k dk = T_{zz}^{\text{applied}} = \frac{e^{-\varpi^2/\varpi_0^2}}{\pi\varpi_0^2} F_o \cos(2\pi ft) ,\quad (11.96)$$

which can be inverted¹¹ to give

$$\alpha(k) = \beta(k) = -\frac{1}{4\pi\mu} e^{-k^2\varpi_0^2/4} F_o \cos(2\pi ft) .\quad (11.97)$$

Inserting this into the Eqs. (11.94) for the displacement, and then evaluating the expansion $\Theta = \nabla \cdot \boldsymbol{\xi} = \xi_{z,z} + \varpi^{-1}(\varpi\xi_{\varpi})_{,\varpi}$, we obtain

$$\Theta = -4\nu \int_0^{\infty} \alpha(k) e^{-kz} J_0(k\varpi) k dk .\quad (11.98)$$

Side Remark: As in electrostatics and magnetostatics, so also in elasticity theory, one can solve an elastostatics problem using Green's functions instead of separation of variables. We explore this, for our applied Gaussian force, in Ex. 11.26 below. For greater detail on Green's functions in elastostatics and their applications, from an engineer's viewpoint, see Johnson (1985). For other commonly used solution techniques see Box 11.3.

¹¹The inversion and the subsequent evaluation of the integral of $(\nabla\Theta)^2$ are aided by the following expressions for the Dirac delta function: $\delta(k - k') = k \int_0^{\infty} J_0(k\varpi) J_0(k'\varpi) \varpi d\varpi = k \int_0^{\infty} J_1(k\varpi) J_1(k'\varpi) \varpi d\varpi$.

Thermoelastic Noise Spectral Density

Returning to the mirror-noise problem that motivated our calculation: It is straightforward to compute the gradient of the expansion (11.98), square and integrate to get the spectral density $S_q(f)$ [Eq. (11.92)]. The result is

$$S_q(f) = \frac{8(1 + \nu)^2 \kappa \alpha^2 k_B T^2}{\sqrt{2\pi} c_V^2 \rho^2 \varpi_o^3 (2\pi f)^2}. \quad (11.99)$$

Early plans for advanced LIGO gravitational wave detectors called for mirrors made of high-reflectivity dielectric coatings on sapphire crystal substrates. Sapphire was chosen because it can be grown in giant crystals with very low impurities and dislocations and resulting low thermal noise. However, the thermoelastic noise (11.99) in sapphire turns out to be uncomfortably high. With sapphire's $\nu = 0.29$, $\kappa = 40 \text{ W m}^{-1} \text{ K}^{-1}$, $\alpha = 5.0 \times 10^{-6} \text{ K}^{-1}$, $c_V = 790 \text{ J kg}^{-1} \text{ K}^{-1}$, $\rho = 4000 \text{ kg m}^{-3}$, and a light-beam radius $\varpi_o = 4 \text{ cm}$ and room temperature $T = 300 \text{ K}$, Eq. (11.99) gives for the noise in a bandwidth equal to frequency:

$$\sqrt{f S_q(f)} = 5 \times 10^{-20} \text{ m} \sqrt{\frac{100 \text{ Hz}}{f}}. \quad (11.100)$$

While this looks like a small number, it would have been mildly unpleasant at the lowest frequencies of interest. For that reason, and because of the birefringence of sapphire, which could cause technical problems, a decision was made to switch to fused silica for the advanced LIGO mirrors.

EXERCISES

Exercise 11.25 *Derivation and Practice: Evaluation of Elastostatic Force in Cylindrical Coordinates*

Derive Eqs. (11.93) for the cylindrical components of the internal elastostatic force per unit volume $\mathbf{f} = (K + \frac{1}{3}\mu)\nabla(\nabla \cdot \boldsymbol{\xi}) + \mu\nabla^2\boldsymbol{\xi}$ in a cylindrically symmetric situation.

Exercise 11.26 *** *Example: Green's Function for Normal Force on Half-Infinite Body*

Suppose that a stress $T_{zj}^{\text{applied}}(\mathbf{x}_o)$ is applied on the face $z = 0$ of a half-infinite elastic body (one that fills the region $z > 0$). Then by virtue of the linearity of the elastostatics equation $\mathbf{f} = (K + \frac{1}{3}\mu)\nabla(\nabla \cdot \boldsymbol{\xi}) + \mu\nabla^2\boldsymbol{\xi} = 0$ and the linearity of its boundary conditions, $T_{zj}^{\text{internal}} = T_{zj}^{\text{applied}}$, there must be a Green's function $G_{jk}(\mathbf{x} - \mathbf{x}_o)$ such that the body's internal displacement $\boldsymbol{\xi}(\mathbf{x})$ is given by

$$\boxed{\boldsymbol{\xi}_j(\mathbf{x}) = \int G_{jk}(\mathbf{x} - \mathbf{x}_o) T_{zk}^{\text{applied}}(\mathbf{x}_o) d^2x_o}. \quad (11.101)$$

Here the integral is over all points \mathbf{x}_o on the face of the body ($z = 0$), and \mathbf{x} can be anywhere inside the body, $z \geq 0$.

- (a) Show that, if a force F_j is applied on the body's surface at a single point, the origin of coordinates, then the displacement inside the body is

$$\xi_j(\mathbf{x}) = G_{jk}(\mathbf{x})F_k . \quad (11.102)$$

Thus, the Green's function can be thought of as the body's response to a point force on its surface.

- (b) As a special case, consider a point force F_z directed perpendicularly into the body. The resulting displacement turns out to have cylindrical components¹²

$$\begin{aligned} \xi_z &= G_{zz}(\varpi, z)F_z = \frac{(1+\nu)}{2\pi E} \left[\frac{2(1-\nu)}{\varpi} + \frac{z^2}{\varpi^3} \right] F_z , \\ \xi_\varpi &= G_{\varpi z}(\varpi, z)F_z = -\frac{(1+\nu)}{2\pi E} \left[\frac{1-2\nu}{\varpi+z} - \frac{z}{\varpi^2} \right] F_z . \end{aligned} \quad (11.103)$$

It is straightforward to show that this displacement does satisfy the elastostatics equations (11.93). Show that it also satisfies the required boundary condition $T_{z\varpi}(z=0) = -2\mu\Sigma_{z\varpi} = 0$.

- (c) Show that for this displacement, $T_{zz} = -K\Theta - 2\mu\Sigma_{zz}$ vanishes everywhere on the body's surface $z=0$ except at the origin $\varpi=0$ and is infinite there. Show that the integral of this normal stress over the surface is F_z , and therefore $T_{zz}(z=0) = F_z\delta_2(\mathbf{x})$ where δ_2 is the two-dimensional Dirac delta function in the surface. This is the second required boundary condition.
- (d) Plot the integral curves of the displacement vector $\boldsymbol{\xi}$ (i.e. the curves to which $\boldsymbol{\xi}$ is parallel) for a reasonable choice of Poisson's ratio ν . Explain physically why the curves have the form you find.
- (e) One can use the Green's function (11.103) to compute the displacement $\boldsymbol{\xi}$ induced by the Gaussian-shaped pressure (11.90) applied to the body's face, and to then evaluate the induced expansion and thence the thermoelastic noise; see Braginsky, Gorodetsky and Vyatchanin (1999), or Liu and Thorne (2000). The results agree with those (11.98) and (11.99) deduced using separation of variables.

Bibliographic Note

Elasticity Theory was developed in the 18th, 19th and early 20th centuries. The classic, culminating advanced textbook from that era is Love (1927), which is available as a Dover

¹²For the other components of the Green's function, written in Cartesian coordinates (since a non-normal applied force breaks the cylindrical symmetry), see Eqs. (8.18) of Landau and Lifshitz (1986).

Box 11.5
Important Concepts in Chapter 11

• **Foundational Concepts**

- Displacement vector field $\boldsymbol{\xi}$, Sec. 11.2.1
- Irreducible tensorial parts of a tensor, Box 11.2
- Irreducible tensorial parts of $\mathbf{W} \equiv \nabla \boldsymbol{\xi}$: expansion Θ , rotation \mathbf{R} and shear $\boldsymbol{\Sigma}$, Sec. 11.2.2 and Box 11.2
- Strain tensor, $\mathbf{S} = (\text{symmetric part of } \nabla \boldsymbol{\xi}) = \boldsymbol{\Sigma} + \frac{1}{3}\Theta \mathbf{g}$, Sec. 11.2.2
- Hooke's law and Young's modulus E , Secs. 11.1, 11.3.2 and 11.4
- Failure of Hooke's law: Proportionality limit, elastic limit, yield point, rupture point, 11.3.2
- Dislocations in a crystal and their movement causing inelastic deformation, Fig. 11.6
- Stress tensor and its divergence as force density, Sec. 11.3.1
- The Pascal as a unit of stress, Sec. 11.3.1
- Bulk and shear moduli K, μ ; elastic stress tensor $\mathbf{T} = -K\Theta \mathbf{g} - 2\mu \boldsymbol{\Sigma}$, Sec. 11.3.3
- Elastic energy (energy of deformation), Sec. 11.3.4
- Thermal expansion and thermoelastic stress, Sec. 11.3.5
- Molecular origin of elastic moduli and orders of magnitude, Sec. 11.3.6
- Elastic force on a unit volume, $\mathbf{f} = -\nabla \cdot \mathbf{T} = (K + \mu/3)\nabla(\nabla \cdot \boldsymbol{\xi}) + \mu \nabla^2 \boldsymbol{\xi}$, Sec. 11.3.3
- Connection Coefficients and their use in cylindrical and spherical coordinate systems, Sec. 11.8

• **Elastostatic Equilibrium**

- Navier-Cauchy equation for stress balance, Sec. 11.3.7
- Boundary condition $T_{ij}n_j$ continuous, Sec. 11.3.7
- Methods of solving Navier-Cauchy equation: Box 11.3
- Dimensional reduction via method of moments, and application to rods, beams and fibers, and to plates: Secs. 11.5, 11.7
- The flexural rigidity D of a rod, beam, or fiber, and its relationship to the shear and torque associated with bending Eqs. (11.42)
- Buckling and bifurcation of equilibria: Sec. 11.6

reprint. An outstanding, somewhat more modern advanced text is Landau and Lifshitz (1986) — originally written in the 1950s and revised in a third edition in 1986, shortly before Lifshitz's death. This is among the most readable textbooks that Landau and Lifshitz wrote,

and is still widely used by physicists in the early 21st century.

Some significant new insights, both mathematical and physical, have been developed in recent decades; for example, catastrophe theory and its applications to bifurcations and stability, practical insights from numerical simulations, and practical applications based on new materials such as carbon nanotubes. For a modern treatment that deals with these and much else from an engineering viewpoint, we strongly recommend Ugural and Fenster (2012). For a fairly brief and elementary modern treatment, we recommend Part III of Lautrup (2005). Other good texts that focus particularly on solving the equations for elastostatic equilibrium include Southwell (1941), Timoshenko and Goodier (1970), Gladwell (1980), Johnson (1985), Boresi and Chong (2000), and Slaughter (2002); see also the discussion and references in Box 11.3.

Bibliography

Braginsky, V. B., Gorodetsky, M. L., and Vyatchanin, S. P. 1999. “Thermodynamical fluctuations and photo-thermal shot noise in gravitational wave antennae” *Physics Letters A*, **264**,1.

Chandrasekhar, S. 1962. *Ellipsoidal Figures of Equilibrium*, New Haven: Yale University Press.

Boresi, Arthur R. and Chong, Ken P. 2000. *Elasticity in Engineering Mechanics*, New York: Wiley.

Gladwell, G. M. L. 1980. *Contact Problems in the Classical Theory of Elasticity*, Alphen aan den Rijn: Sijthoff and Noordhoff.

Fortere, Yo el, Skothelm, Jan M., Dumals, Jacques, and Mahadevan, L. 2005. “How the Venus Flytrap Snaps”, *Nature*, **433**, 421.

Jackson, J. D. 1999. *Classical Electrodynamics*, New York: Wiley.

Johnson, K. L. 1985. *Contact Mechanics*, Cambridge: Cambridge University Press.

Constantinescu, Andrei and Korsunsky, Alexander. 2007. *Elasticity with Mathematica*, CUP.

Kapner, D.J., Cook, T.S., Adelberger, E.G., Gundlach, J.H., Heckel, B.R., Hoyle, C.D., and Swanson, H.E. 2008, “Tests of the Gravitational Inverse-Square Law Below the Dark-Energy Length Scale”, *Phys. Rev. Lett*, **100**, 041101.

Landau, L. D., and Lifshitz, E. M. 1986. *Elasticity*, Third Edition, Oxford: Pergamon.

Levin, Yu. 1998. “Internal thermal noise in the LIGO test masses: a direct approach” *Physical Review D*, **57**,659–663.

- Liu, Y. T., and Thorne, K. S. 2000. “Thermoelastic noise and thermal noise in finite-sized gravitational-wave test masses” *Physical Review D*, in preparation.
- Lautrup B. 2005. *Physics of Continuous Matter*, Bristol and Philadelphia: Institute of Physics Publishing.
- Love, A.E.H. 1927. *A Treatise on the Mathematical Theory of Elasticity*, Cambridge: Cambridge University Press; Reprinted – New York: Dover Publications (1944).
- Marko, John F. and Cocco, Simona 2003. “The Micromechanics of DNA”, *Physics World*, March 2003, pp. 37–41.
- Marsden, Jerold E. and Hughes, Thomas J.R. 1986. *Mathematical Foundations of Elasticity*, Upper Saddle River NJ: Prentice-Hall; Reprinted – New York: Dover Publications(1994).
- Mathews, J. and Walker, R. L. 1965. *Mathematical Methods of Physics*, New York: Benjamin.
- Messiah, A. 1962. *Quantum Mechanics, Vol. II*, Amsterdam: North-Holland.
- Nelson, Philip 2004. *Biological Physics*, San Francisco: W.H. Freeman.
- NIST 2005. National Institute of Standards and Technology, *Final Report on the Collapse of the World Trade Center Towers*, U.S. Government Printing Office, Washington DC; available at <http://www.nist.gov/el/disasterstudies/wtc/> .
- NIST 2008. National Institute of Standards and Technology, *Final Report on the Collapse of the World Trade Center Building 7*, U.S. Government Printing Office, Washington DC; available at <http://www.nist.gov/el/disasterstudies/wtc/> .
- Southwell, R.V. 1941. *An Introduction to the Theory of Elasticity for Engineers and Physicists*, Second Edition, Oxford: Clarendon Press; Reprinted – New York: Dover Publications.
- Slaughter, William S. 2002. *The Linearized Theory of Elasticity*, Boston: Birkäuser.
- Todhunter, Isaac and Pearson, Karl. 1886. *A History of the Theory of Elasticity and of the Strength of Materials, from Galilei to the Present Time (1886)*, Cambridge: Cambridge University Press.
- Thorne, K.S. 1980. “Multipole Moments in General Relativity” *Rev. Mod. Phys.*, **52**, 299.
- Timoshenko, S. and Goodier, J. N. 1970. *Theory of Elasticity*, Third Edition, New York: McGraw-Hill.
- Ugural, Ansel C. and Fenster, Saul, K. 2012. *Advanced Mechanics of Materials and Applied Elasticity*, Fifth Edition, Upper Saddle River NJ: Prentice-Hall.

Xing, Xiangjun, Goldbart, Paul M. and Radzihovsky, Leo 2007. “Thermal Fluctuations and Rubber Elasticity”, *Phys. Rev. Lett.* **98**, 075502.

Yeganeh-Haeri, A., Weidner, D. J. & Parise, J. B. 1992. *Science*, **257**, 650.

Wagner, T.A., Schlamminger, S., Gundlach, J.H., and Adelberger, E.G. 2013. “Torsion-Balance Tests of the Weak Equivalence Principle”, *Class. Quant. Grav.*, in press.

Weld, David M., Xia, Jing, Cabrera, Blas, and Kapitulnik, Aharon. 2008. “A New Apparatus for Detecting Micron-Scale Deviations from Newtonian Gravity”, *Phys. Rev. D* **77**, 062006.

Wolgemuth, Charles W., Powers, Thomas R., and Goldstein, Raymond E. 2000. “Twirling and Whirling: Viscous Dynamics of Rotating Elastic Filaments”, *Phys. Rev. Lett.* **84**, 1623–1626.